NMRF/RR/01/2020

RESEARCH REPORT

Super Cyclone "*Amphan*": Verification of NCMRWF Model Forecasts

**Mohana S. Thota, Sushant Kumar, Anumeha Dube, S. Karunasagar,
Harvir Singh, Indira Rani S., Sumit Kumar, Amar Jyothi K.,
Abhijit Sarkar, S. Kiran Prasad, Paromita Chakraborty,
Imranali M. Momin, Arulalan T., Preveen Kumar D.,
Raghavendra Ashrit and E.N. Rajagopal**

June 2020

**National Centre for Medium Range Weather Forecasting
Ministry of Earth Sciences, Government of India
A-50, Sector-62, NOIDA-201 309, INDIA**

Super Cyclone "*Amphan*": Verification of NCMRWF Model Forecasts

**Mohana S. Thota, Sushant Kumar, Anumeha Dube, S. Karunasagar, Harvir Singh,
Indira Rani S., Sumit Kumar, Amar Jyothi K., Abhijit Sarkar, S. Kiran Prasad,
Paromita Chakraborty, Imranali M. Momin, Arulalan T., Preveen Kumar D.,
Raghavendra Ashrit and E.N. Rajagopal**

June 2020

**National Centre for Medium Range Weather Forecasting
Ministry of Earth Sciences
A-50, Sector 62, Noida-201 309, INDIA**

Ministry of Earth Sciences
National Centre for Medium Range Weather Forecasting
Document Control Data Sheet

1	Name of the Institute	National Centre for Medium Range Weather Forecasting
2	Document Number	NMRF/RR/01/2020
3	Date of Publication	June 2020
4	Title of the document	Super Cyclone "Amphan": Verification of NCMRWF Model Forecasts
5	Type of the document	Research Report
6	Number of pages, figures, and Tables	51 Pages, 31 Figures and 4 Tables
7	Authors	Mohana S. Thota, Sushant Kumar, Anumeha Dube, S. Karunasagar, Harvir Singh, Indira Rani S., Sumit Kumar, Amar Jyothi K., Abhijit Sarkar, S. Kiran Prasad, Paromita Chakraborty, Imranali M. Momin, Arulalan T., Preveen Kumar D., Raghavendra Ashrit and E.N. Rajagopal
8	Originating Unit	National Centre for Medium Range Weather Forecasting (NCMRWF)
9	Abstract (brief)	This report gives a detailed summary of the verification of the NCMRWF model forecasts during the recent Super Cyclone (SUCS) 'Amphan' during (16-21 May2020). The mean (all models) initial position error is 48 km with highest error of 53 km in NCUM-R. The mean (all models) 24-hr track error is around 54 km with highest error of 78 km in NCUM-R. Similarly, the mean track error at 48 and 72 hr is 114 km and 177 km respectively. NEPS-G has highest error of 133 km and 197 km at 48 and 72 hr lead time respectively. The forecast track errors computed during the initial days (13-15 May 2020) are much smaller when compared to those computed after the naming of the cyclone. During the initial days it was in the range of 85-93 km while during the later stage of cyclone it was in the range of 102-157 km in 48 hr forecast. The landfall position errors range from 50-80 km in all forecasts made after 12 UTC on 18 May 2020. The error in the landfall time is low in all the forecasts made after 00 UTC of 18th May 2020 and in the range of -03:30 hr to +01:30 hr. Ensemble based strike probability is verified using standard procedures of Reliability Diagram and ROC curves. The results demonstrate the benefits of 23 member ensemble against the 12 member ensemble in NEPS-G. Additionally, the impact of high resolution NEPS-R at 4 km is also demonstrated in terms of improved reliability as against the NEPS-G at 12 km resolution.
10	References	12
11	Security classification	Unrestricted
12	Distribution	General

Table of contents

Abstract

This report gives a detailed summary of the verification of the NCMRWF model forecasts during the recent (16-21 May2020) Super Cyclone (SUCS) ‘***Amphan***’. The verification of forecast tracks and intensity is presented for NCMRWF Unified Model (NCUM-G) (12 km grid resolution) for both 00 UTC and 12 UTC, NCMRWF Ensemble Prediction System NEPS-G mean (12 km grid resolution) and Regional models, NCUM-R and NEPS-R (4 km grid).

Verification of deterministic and ensemble mean forecast tracks is expressed in terms of track forecast errors, initial position, landfall position, and landfall time errors. The mean (all models) initial position error is 48 km with highest error of 53 km in NCUM-R. The mean (all models) 24-hr track error is around 54 km with highest error of 78 km in NCUM-R. Similarly, the mean track error at 48 and 72 hr are 114 km and 177 km respectively. NEPS-G has highest error of 133 km and 197 km at 48 and 72 hr lead time respectively. The forecast track errors computed during the initial days (13-15 May 2020) are much smaller when compared to those computed after the naming of the cyclone. During the initial days it was in the range of 85-93 km while during the later stage of cyclone it was in the range of 102-157 km in 48 hr forecast. The landfall position errors range from 50-80 km in all forecasts made after 12 UTC of 18 May 2020. The error in the landfall time is low in all the forecasts made after 00 UTC of 18 May 2020 and in the range of -03:30 hr to +01:30 hr.

Ensemble based forecast tracks are used to construct the tropical cyclone strike probabilities. The verification of strike probability is presented using standard procedures using Reliability Diagram and ROC curves to demonstrate the benefits of 23 member ensemble as against the 12 member ensemble in NEPS-G. Additionally, the impact of high resolution NEPS-R at 4 km is also demonstrated in terms of improved reliability as against the NEPS-G at 12 km resolution. The enhanced active phase of MJO as seen in NEPS-G forecasts is favouring the sustainment of cyclone.

1. Introduction

This report gives a detailed summary of the verification of the National Centre for Medium Range Weather Forecast (NCMRWF) model forecasts during the recent (16-21 May2020) Super Cyclone (SUCS) '***Amphan***'). The North Indian Ocean cyclone season's (April to November) first tropical cyclone *Amphan* is a Super Cyclone, which caused widespread damage in the Eastern parts of India during May 2020. According to India Meteorological Department (IMD) the cyclone was the strongest tropical cyclone to occur in the Bay of Bengal since the 1999 Odisha Super cyclone. The landfall of this cyclone occurred over West Bengal, causing widespread damage. It was considered the strongest to hit the region in over a decade killing at least 86 people in West Bengal. Coastal areas in Odisha, particularly Paradeep, received huge amounts (>200 mm) of 24 hr accumulated rainfall during 19-20 May 2020 (IMD tropical cyclone bulletin of 20 May 2020).

1.1 NCMRWF Unified Modelling System

The verification of forecast tracks and intensity is presented for two sets of global and regional models; (i) NCMRWF Unified global model (NCUM-G) and its ensemble prediction system (NEPS-G) (12 km resolution); (ii) regional model NCUM-R and its ensemble NEPS-R (4 km resolution) for 00 and 12 UTC based model predictions. Forecast tracks and verification is presented for model predicted tracks based on the IMD best track data. Table 1 summarizes the model configurations operational at NCMRWF. Details on the model parameterizations, Data assimilation etc., can be found in Sumit Kumar et al. (2018).

2. Meteorological Conditions and Phenology of the Super Cyclone "Amphan"

Super cyclone 'Amphan' originated from a low-pressure area that developed over the Southeastern Bay of Bengal on 15th May 2020. The spatial patterns of mean sea level pressure (MSLP) and associated surface winds (at 10m level) from the NCUM global model analysis depicts the omnipresence of low pressure and cyclonic circulation over south eastern parts of Bay of Bengal (BoB) (Figure 1a and Figure 1b). The area of low pressure was situated in a more favorable environment comprising of low vertical shear regime (Figure 1c) and warm sea-surface temperature (SST) (Figure 1d). Observed NOAA SST anomalies during 15th May 2020 (Figure 1d) shows warm temperature anomalies (>2 K) over most of the Bay of Bengal region. The combined effect of low vertical shear and the warm SSTs acted in initiating the conducive environment for the cyclone movement and sustainment. In addition, satellite derived sea level anomaly (SLA), which indicates the eddy circulation is also shown for the period 15-17 May 2020 in Figure 1(e)-(g). Here, the positive (negative) SLA over BoB depict warm (cold) core eddies indicates the deep (shallow) thermoclines. The presence of warm core eddies enhances the cyclone intensification (Shay et al., 2000).

The basic phenology of the cyclone indicates that on 16th May 2020 at 00 UTC the low-pressure area had developed into depression and designated as BB01 while it was located about 1,100 km to the south of Paradeep, Odisha. Six hours later IMD upgraded the system to a deep depression. This well marked depression, which started moving northwards, continually organized and further strengthened to become a cyclonic storm. On 17th May 2020 around 09 UTC Amphan underwent rapid intensification due to the presence of more conducive upper level winds and transformed into severe cyclonic storm with winds ranging from 140-215 km/h (85-130 mph). These winds are equivalent to a Category 4 hurricane on the Saffir-Simpson scale (https://en.wikipedia.org/wiki/Saffir-Simpson Scale) (Saffir, 1973; Simpson, 1974). Furthermore, IMD upgraded Amphan to an extremely severe cyclonic storm based on their cyclone intensity scale. The broad storm was characterized by cloud bands extending more than 1,110 km and a sharply outlined 18-20 km wide eye. On 18th May 2020, the super cyclonic storm was over west central Bay of Bengal and moved north-northeastwards and lay centered around 16.5°N and 86.9°E at 11:30 hrs IST of 19th May 2020. According to Joint Typhoon Warning Center (JTWC), the cyclone “explosively intensified” from category 1 to category 4 equivalent in just 6 hours. On 19th May 2020, IMD upgraded Amphan to a super cyclonic storm with 3-minute sustained winds of 240 km/h and a minimum central pressure of 925 hPa. The Super cyclonic storm continued its movement northeastwards and landfall occurred on 20th May 2020. As it moved further inland, it rapidly weakened. Just six hours after landfall, the cyclone downgraded into Category 1-equivalent cyclone and became disorganized.

3. Meteorological observations – Space borne, Buoy and Radar

NCMRWF routinely assimilates both conventional and satellite observations in the global, regional and ensemble prediction systems. During Tropical cyclones, assimilation of observations in the vicinity of cyclone plays a crucial role in the accurate representation of the cyclone in the model analysis. A brief overview of the observations assimilated during the cyclone Amphan is provided in this section.

Though various observations are assimilated routinely, surface observations over the ocean play vital role during cyclone period. Conventional observations from Buoy and Ship and scatterometer sea surface winds from active satellite payloads are inevitable for the accurate representation of cyclone in the initial analysis. Apart from the above observations, Tropical Cyclone Vitals (TC-Vitals) are also assimilated for the vortex relocation and bogusing process in the models. Figure 2 shows the scatterometer sea surface winds assimilated in the NCUM-G during the life span of Amphan cyclone during different data assimilation cycles. The scatterometer winds are assimilated particularly in all 06 and 18 UTC assimilation cycles. Generally, the scatterometer passes over the Indian seas are few or nil during 00 and 12 UTC, mainly because all the three operational scatterometer missions (ASCAT-A, ASCAT-B and ScatSat-1) are in the morning orbit. A well-defined cyclonic structure can be seen in the assimilated scatterometer winds at 06 UTC of 16 and 17 May, 12 UTC of 17 May and 06 UTC of 20 May 2020. Partial structure can be seen in different 18 UTC assimilation cycles.

Figure 3 and 4 shows the assimilated pressure observations from Buoy during the period of Amphan cyclone. Each row in Figure 3 and Figure 4 represents the observations assimilated during four different assimilation cycles during 16-17 May and 18-20 May 2020, respectively. It is clear from Figure 3 and Figure 4 that from 06 UTC of 16 May 2020 onwards, the Buoy observations accurately reported the low pressure (circled in red) and the same had been assimilated in the system. Figure 5 shows the location of surface pressure from the TC-Vitals assimilated during the period of Amphan cyclone. Figure 5 accurately represents the cyclone location and the model also benefitted from the assimilation of the same in predicting the track of the cyclone well in advance as discussed in sections 7 and 8.

Doppler Weather Radar (DWR) observations also play a crucial role in studying the movement and evolution of the cyclone. Time series of the maximum radar reflectivity observed by the DWR situated at Kolkata (VECC) on the day of cyclone Amphan landfall i.e., 20th May 2020 is showed in Figure 6a. Maximum reflectivity of around 70 dBz is observed at two different peaks. Clear indication of deep convective clouds having large reflectivity values are seen throughout the day during the landfall of the cyclone. Spatial maps of radar derived radial winds before ~08:20 UTC (Figure 6b) and after landfall ~10:50 UTC (Figure 6c) was seen flowing inward towards the land before making landfall. In addition to the reflectivity and radial winds, surface rainfall intensity (mm/hr) obtained from DWR Kolkata at 09:32 UTC during the cyclone landfall shows more than 150 mm/hr around the eye walls (Figure 6d). Rainfall bands of magnitude ~100 mm/hr near the eye are also observed. The structure of the cyclone and convective rain spiral bands are seen in both the reflectivity time series and surface rainfall intensity map. The rainfall was computed using the calibrated constants. In conjunction with the observations, the spatial distribution of rainfall during 16-21 May 2020 seen in satellite and rain gauge merged IMD-NCMRWF rainfall product (Mitra et al., 2009) is also shown in Figure 7. Evolution of the cyclone as noticed by movement of rainfall band, intensification during 17-18 May 2020 and landfall is clearly observed. Large amounts of rainfall (>64 cm) over southeast BoB during the evolution of Amphan cyclone is well seen from the merged data set (Figure 7). The 7-day average rainfall shows the entire BoB is convectively active during this period consisting with the presence of warm SSTs over BoB.

4. NCUM Global and Regional Analysis

The space-time evolution of Amphan cyclone in NCUM global and regional analysis during 00 and 12 UTC are for MSLP and 850 hPa winds are shown in Figure 8 and Figure 9 respectively. Observed cyclone track (black solid line) is also indicated in each of the panels to verify the cyclone position in the model analysis. In order to be brief, here the performance of NCUM-G analysis and forecasts during the cyclone is discussed only in terms of MSLP and 850 hPa level winds. It is seen that global and regional analysis represent the well-marked low-pressure system and its intensification fairly well, during the course of the cyclonic storm. On 16-17th May 2020, within a span of 12 hours or less, the system became more distinct as it gradually strengthens into a depression, due to its stay over warm oceans for relatively longer periods, with spiral bands of deep convective clouds surrounding the system's low-level center as evidenced by the stream lines (Figure 8 and Figure 9). Despite having different resolutions, on all the days (i.e., 16-20 May 2020) intensity of the cyclone, in terms of wind speed in both global (Figure 8) and regional (Figure 9) analysis are agreeing well. Enhanced circular isobars and wind speeds in both global and regional analysis indicates the rapid intensification of the storm on 17th May 2020. A close correspondence in the movement and land fall of the system is seen in both the analysis.

5. NCUM Global and Regional Forecasts

In this section, a brief description of global and regional forecasts during the Amphan cyclone period is discussed. When compared with the global reanalysis, the 24 hr (Day-1) forecast of

MSLP and 850 hPa winds (Figure 10 and Figure 11 respectively) from the global NCUM predicts the well-marked depression on 16th May 2020, rapid intensification of the storm on 17th May 2020 and steady movement on the next couple of days and landfall on 20th May 2020 agree well. The intensity of the cyclone as seen from the 850 hPa low-level winds are also well predicted in global model forecasts (Figure 11). Day-1 global NCUM forecasts on 18th May 2020 show the North-west ward movement of the system and landfall occurrence on the 20th May 2020. Subsequently Day-3 forecasts show the system has made further inward movement towards land and located over west Bengal. As it moved further inland, it rapidly weakened. Just six hours after landfall, the cyclone downgraded into Category 1 equivalent cyclone and became disorganized. On the other hand, the regional NCUM forecasts slightly overestimate the intensity at all the forecast times. Further, in the regional NCUM, the centre of the cyclone is slightly located south-eastward compared to the respective analysis and the IMD best track position (black solid line). This intensity overestimation in the regional NCUM Day-1 forecast is also evident in the winds (Figure 11). It is interesting to note that, cyclone movement meanders in the regional model forecast compared to best track with the lead time. For example, the centre of the cyclone is situated on the westward side of the best track position during the rapid intensification period (on 17th May 2020), whereas it moved to east side of the track in the subsequent days.

6. NCMRWF Ensemble Prediction System (NEPS) Forecasts

6.1 Global Ensemble Forecasts (NEPS-G)

NEPS-G control analysis of mean sea level pressure (MSLP) (Figure 12(a)) shows that the centre of cyclone Amphan lies near Odisha coast at 00 UTC of 20th May 2020. The red contours depict the ensemble mean MSLP and the spread between the ensemble members are shown in blue shade. The drop in ensemble-mean MSLP is over-predicted by NEPS-G in Day-3 (Figure 12b). It is better predicted in Day-5 forecast (Figure 12c). The spread or disagreement is higher in magnitudes of the isobars in Day-3 forecast whereas spread is higher in the location of the contours in Day-5 forecast.

The wind analysis at 850 hPa (Figure 13a) shows a well-defined vortex near the coast of Odisha and West Bengal at 00 UTC 20th May 2020. The Day-3 predicted ensemble mean wind (Figure 13b) shows strong cyclonic circulation associated with TC Amphan over Bay of Bengal with a spread of 14-16 m/s. The location of the vortex centre in Day-3 forecast is shifted north-eastward from the location of the analysis. Day-5 predicted ensemble mean wind shows that the location of vortex is at the south of the analysis vortex with slightly higher ensemble spread (Figure 13c).

Figure 14(a) depicts the 24-hourly accumulated rainfall from IMD-NCMRWF merged satellite gauge product (Mitra et al., 2009) for 20th and 21st May 2020 associated with cyclone Amphan. Day-5 predicted ensemble mean 24 hr accumulated precipitation (Figure 14b) shows moderate (4-8 cm) rainfall with a few patches of heavy (8-16 cm) rainfall over West Bengal, Bangladesh, and Myanmar. Light (2-4 cm) rainfall is predicted over entire eastern India. There was a prediction of 50-75% probability of rainfall valid at 03 UTC 21st May 2020 exceeding 65.5 mm/day (Figure 14c) in these locations in Day-5 forecast. However, the probability of precipitation exceeding 115 mm/day and 195 mm/day was predicted to be above 25% and below 25% respectively (Figure 14d and 14e).

Figure 15 shows Ensemble meteogram or EPSgram for three locations - North 24-Parganas, South 24-Parganas and Kolkata during TC Amphan for the model run based on 17th May 2020. The boxes show a range of 25-75% percentile values and whiskers show the range between minimum and maximum values. The red line joins median values. The figure shows that a few ensemble members predicted wind speed at 10 m greater than 30 m/s and MSLP less than 940 hPa over South 24-Parganas on 20th May 2020. More than 25% members predicted peak rainfall greater than 90 mm/6 hr over South 24-Parganas on that day.

6.2 Regional Ensemble Forecasts (NEPS-R)

The Super Cyclone Amphan made landfall between 10 and 11 UTC on 20th May 2020 and the PQPF of NEPS-R for Day-1 and Day-2 shown in Figures 16 and 17 indicate that NEPS-R was unable to predict the precipitation greater than 16 cm in its mean forecast primarily due to the spread in location of prediction among the members. However, the model has done well in predicting the heavy rain of >16cm in Day-2 forecast. The other ranges of rainfall were well captured by NEPS-R on Day-1 and Day-2 and are in good agreement with the observed rainfall. The rainfall band over northcentral Bay of Bengal on 21st May was well predicted in Day-1 forecast but was not captured well in Day-2. Further, the probability of occurrence of rainfall >19.5cm is 30-50% in both Day-1 and Day- 2 but spread over a larger area in Day-2 forecast. The probabilities for other thresholds of rainfall are similar but spread over a slightly larger area in Day-2 forecast than in Day-1 for the thresholds >6.55cm and >11.5cm, indicating a better Day-2 rainfall forecast.

Figure 18a shows the analysed MSLP of over Bay of Bengal, with the cyclone over Head Bay close to Odisha coast on 00 UTC of 20th May 2020. The black contours depict the ensemble mean MSLP and the spread between the ensemble members are shown in blue shade. The drop in ensemble-mean MSLP is overpredicted by NEPS–R in Day-2 (Figure 18b). It is better predicted in Day-1 forecast (Figure 18c). The spread or disagreement is more and over a larger area in Day-2 in comparison to Day-1 around the centre of the system.

Figure 19a and 19b illustrates the observed radar winds and NEPS-R Day-1 forecast of 10 m winds. It is seen from the Figure 19 that NEPS-R predicted the intensity well in-terms of wind speed. The maximum winds of around 24 m/s was predicted by NEPS-R against a 30 m/s observed by the radar. However, considering the fact that model predicted winds are at 10 m whereas the radar winds are at a height of about 50 -250 m, the friction near the surface at 10 m height would be more and that would have reduced the wind speed at that height in NEPS-R. So, the wind speed predicted by NEPS-R could very well be at par with actual winds at 10 m.

7. Track Forecasts and its Verification

7.1 The bi-variate TC Tracker

The UK Met Office bi-variate approach to tracking TCs is used in the real-time to track the location of the Super Cyclone ‘Amphan’. The bi-variate method identifies TCs by examination of the 850 relative vorticity field but then fixes the TC center to the nearest local MSLP minimum (Heming, 2017). The key advantage of the method is that it gives a strong indication of the approximate centre of the TC even for weak systems and does not depend on the ‘*TC-Vitals*’ information for tracking.

7.2 Observed and Predicted Tracks (00 and 12 UTC)

Track predictions obtained for the cyclone ‘Amphan’ from NCUM-G and NCUM-R for the various initial conditions (ICs) from 16-20 May 2020 during 00 and 12 UTC are shown in Figure 20. Though the cyclone track predictions from both NCUM model versions (global and regional) depicts slight discrepancies with varying ICs when compared with the IMD best track (black curve), most of the track forecasts indicate the cyclone landfall over West Bengal and Bangladesh regions. When compared with IMD track, cyclone track prediction is more accurate and consistent in Day-1 (green) and Day-2 (purple) track forecasts in both NCUM-G and NCUM-R which were initialised on 18th and 19th May 2020, respectively. Track forecast based on 00 and 12 UTC of 16th May 2020 in NCUM-G (and 12 UTC NCUM-R) indicates highest error, with track being much to the east of observed track. Similarly, the track forecast based on 17th May also is shifted eastwards; however, it is an improved track compared to the track predicted based on 16th May.

7.3 Forecast Track Errors

The NCUM-G, NEPS-G and NCUM-R tracks based on 00 and 12 UTC forecasts from 13-20 May 2020 have been used in the verification. Table 2 summarizes the track errors at different lead times. The track error components of the direct position error (DPE), along track error (ATE) and cross track error (CTE) are shown in Figure 21. It is noted that the early forecasts during 16th and 17th May 2020 predicted the track much to the east of the observed track (Figure 19), which is clearly reflected in high CTE values at higher lead times. The mean initial position error is lowest in NCUM-G at 43 km and highest in NEPS-G at 53 km. The 24 hr DPE ranges between 48-68 km, the 48 hr DPE ranges between 99-133 km and the 72 hr DPE ranges between 153-197 km. DPE computed based on the forecasts for 13-15th May (Table 3) indicate lower values compared to the DPE values based on forecasts during 16-20th May 2020. This possibility suggests higher DPE during and after intensification of the cyclone.

7.4 Forecast Landfall Position and Time Errors

Forecast errors in landfall time and position from NCUM-G and NCUM-R is showed in Table 4. Forecasts made on 16th May 2020 had relatively large errors both in landfall position (>200 km) and time of over 7-11 hours (early). The time error has reduced to 1.3-7 hours (early) for forecasts based on 17th May 2020 IC, and the landfall position errors are also lower. Nevertheless, the forecasts made after 00 UTC 18th May 2020 have extremely low error in both landfall position and time (Table 4). The forecasts from NCUM-R show least error in space and time.

7.5 Forecast Intensity

The minima in SLP and maxima in winds indicate the intensity of the cyclone. The observed and forecast Minimum SLP and Maximum Winds are shown in Figure 22. Delayed peak intensity is evident in all three models. The NCUM-R predicted Minimum SLP based on 16th May 2020 comes close to predicting the observed intensity of 920 hPa on 18th May 2020 at 1800 UTC. However, forecast Maximum Wind is 102 kt is much lower compared to observed 125 kt. It is evident from Figure 22 that the model forecast consistently indicated delayed intensification. The mean absolute error in Minimum SLP and Maximum Wind is shown in Figure 23. Highest SLP errors at 24, 48 and 72 hours are in NCUM-R forecasts. Lowest errors are evident in NCUM-G. At higher lead times of 96 ad 120 hr lowest errors are evident in NEPS-G.

7.6 Forecast Intensity in Global and Regional EPS (NEPS-G v/s NEPS-R)

A comparison of NEPS-G and NEPS-R forecast intensities is given in Figure 24. NEPS-G has 23 members obtained from 11 members of 00 and 11 members from the previous 12 UTC runs and 1 control from the current 00 UTC run. However, for the regional NEPS-R (4 km) there are just 11 members from the 00 UTC cycle. RMSE in the wind speed is presented for the ensemble mean of NEPS-G and NEPS-R in Figure 24. Additionally, a comparison is also provided for NEPS-G ensemble mean constructed without the members from previous 12 UTC cycle (NEPS-G (12mem)), which clearly indicates that NEPS-G (23mem) is slightly better. On the overall, the results indicate significant improvement in NEPS-R in terms of reduced RMSE at almost all lead times.

7.6 Reliability of Global and Regional EPS (RMSE v/s Spread)

When evaluating the reliability of an ensemble prediction system, it is common to compare the root-mean-square error of the ensemble mean to the average ensemble spread. Figure 25 shows the RMSE and Spread for the Maximum wind speed associated with cyclone Amphan at different lead times. NEPS-G has large difference between RMSE and spread (except at higher lead times; after 72 hr). At shorter lead times, i.e., 24, 48 and 72 hr NEPS-R has much reduced difference between RMSE and Spread compared to that in NEPS-G suggesting improved reliability in the NEPS-R cyclone intensity forecasts.

8. Cyclone Strike Probability and its Verification

The tropical cyclone strike probability (Figure 26) is computed based on each ensemble member track forecasts for both NEPS-G and NEPS-R. The NEPS-G forecasts are available till Day-5 (120 hours) whereas the NEPS-R forecasts are available only till Day-3 (72 hours). NEPS-G indicates that the cyclone would cross the coast over West Bengal and Bangladesh coast. The same can be seen in the NEPS-R forecasts after 18th May 2020. The Ensemble Meteograms (EPSGrams) showing the central pressure, wind speed and number of ensemble members predicting the cyclone in the respective category is also presented along with the strike probability. The cyclone strike probability is the probability of locating the cyclone within 120 km distance of the ensemble mean. The shaded region in the Figure 26 shows strike probability. The EPSgrams for all the days show peak intensity (low central pressure and high wind speed) on 06 UTC of 20th May 2020.

8.1 Verification of Strike Probability

Verification of strike probability is presented using ROC and Reliability diagram (attributes diagram). The Reliability diagram (Figure 27) gives a comparison of forecast probability against the observed frequencies. A perfect match will show all points along the diagonal. Points above diagonal suggest underestimation (lower forecast probabilities) while points below the diagonal suggest over estimation (higher forecast probabilities). Generally, verification of probabilistic forecasts is carried out based on large number of cases. The results based on limited number of samples from one single case of cyclone need to be interpreted with caution. In the present case the results are to be understood with focus on impact of 23-members as against 12-members.

The NEPS-G strike probability verification is presented for 12-members (operational; in blue) and 23 member (experimental; in red) lagged ensemble. It is found that the forecast strike probability constructed using 12-member ensemble underestimates. Comparatively, the strike probability constructed using 23-member ensemble shows a perfect match with observed frequencies for forecasts of probability < 0.4. For higher probabilities, there is overestimation which is a desirable change relative to operational forecast. This is also reflected in the ROC curve (Figure 27 right panel). The area under ROC is marginally higher for the 23-member ensemble suggesting higher skill compared to 12-member ensemble.

9. MJO Influence on Super Cyclone Amphan

The Madden Julian Oscillation (MJO) is the dominant intra-seasonal variability, and air-sea interaction and other feedback mechanisms contribute to enhancement and propagation of MJO in the equatorial Indian Ocean regions. MJO was weak (RMM index <1) during the first week of May 2020 and subsequently gained its strength (Figure 28a). During the Amphan cyclone period 15-20 May 2020, i.e., when MJO was situated over Indian Ocean and Maritime continent regions (i.e., Phase 2 and 3) it was active (RMM index > 1) (Figure 28a). The associated Kelvin and Rossby wave activity enhanced the convection over Indian Ocean resulting high cloudiness and inducing the favourable conditions for sustaining the convection and amplification of cyclone.

Figures 28b-c shows the verification of MJO phase and amplitude in ensemble forecasts against NCUM analysis plus observation (black line) based on different initial conditions. Figure 28b shows 10 days forecast (red, light green, dark green colored lines) based on 10th May 2020 initial condition and its verification against analysis (NCUM) marked in black line. The figure indicates that active MJO was in phase 2 and 3 during 11-20 May 2020. Figure 28c is also same as Figure 28b but based on initial condition on 14th May 2020. The NEPS-G members (at least a few) predicted well matched with observed plus analysis amplitude and phase location.

10. Spatial Verification of Cyclone Induced Rainfall Forecasts

10.1 Contiguous Rain Area (CRA) Verification

Accurate rainfall forecast should have good match with observations in terms of location, intensity, and areal distribution. NWP based rainfall forecasts are rarely accurate on all aspects. The traditional verification statistics also fail to provide details about the errors in location, distribution etc., and their contribution to the total forecast errors. With the spatial verification methods, one can get the relation between the neighbouring grid points rather than grid to grid relation match as in traditional verification. Additionally, spatial verification methods assess the feature of interest in the same domain. Contiguous Rain Area (CRA) method (Ebert and McBride, 2000; Ebert and Gallus, 2009; Kuldeep Sharma et al., 2019) aims to verify the properties of forecast entities against the properties of the observation entities. The big advantage of this method is the total error can be decomposed into location, volume, and pattern errors and hence it gives the quality of the matches. The CRA is the union of the forecast and observed rain entities selected based on a user specified isohyet in the observation and forecast. In this study, the CRAs defined by higher thresholds of 40 mm/day are used to better isolate the rain event associated with Super Cyclone Amphan.

Figure 29 shows the CRA verification for NCUM-G Day-3 rainfall forecast with 40 mm threshold. The total common grids in both observed and forecast are 459. It is well known that the number of grids will be less when verification goes from lower threshold to higher threshold. The maximum rainfall in forecast (300.1) is slightly lower than observed (325.8) whereas the average rainfall in forecast (73.7) is slightly higher than observed (68.95) which indicates the model predicted more rainfall over a larger area. The actual forecast has a poor match with RMSE as 86.65 and CC as 0.093. The original forecast was located 1.25° longitude and 0.25° latitude to the northeast of the observed location. The displacement error with 67.3% and pattern error with 30.8% stands as major contributors to the total error whereas the contribution from volume error (2%) is very minimum.

10.2 Method for Object-Based Diagnostic Evaluation (MODE)

The Method for Object-Based Diagnostic Evaluation (MODE), provides an object-based verification for comparing gridded forecasts to gridded observations (Bullock et al., 2016). It answers the question “How similar are the forecast objects to the observed objects according to a variety of descriptive criteria. MODE uses a convolution filter and thresholding to first identify objects in gridded fields. Performance at different spatial scales can be investigated by varying the values of the filter and threshold parameters. Then a fuzzy logic scheme is used to merge objects within a field and match them between the forecast and the observations. Several attributes of the matched objects (location, area, volume, intensity, shape, etc.) are compared to see how similar they are. These are combined to give an "interest value" that summarizes the goodness of the match. MODE may be used in a generalized way to compare any two fields containing data from which objects may be well defined. It has most commonly been applied to precipitation fields and radar reflectivity.

Figure 30 shows the MODE analysis for Day-3 predicted rainfall valid for 21st May 2020. The top two panels show the observed and forecast rainfall. The two panels below compare the 200 mm rainfall objects. Two panels on right show forecast object with observation outline and observation object with forecast outline. The overlap among the objects and misses on eastern edges of objects held to quantify the displacement for 200 mm rainfall object.

From the object-based verification of high intensity rainfall in the cluster pair table shows the overall performance of the NCUM-G forecasts. The centroid distance is quantitative measure of the forecast spatial displacement (centroid distance) which is small 4.41 grid-squares and area ratio is 1.59 (134/84) which shows a rather poor areal extent of forecast 3 days in advance for 12 cm/day object. The total interest 0.96 implies a reasonable match of the forecasts with observations.

11. Representation of Cyclone Amphan in NCMRWF Coupled Model

The air-sea interaction plays crucial for the tropical cyclone intensification; especially the upper ocean provides the heat to the atmospheric boundary layer and the deepening process. In this study, the global Nucleus for European Modeling of the Ocean (NEMO) analysis of temperature and salinity at 0.25x0.25 degree resolution are used to compute the Tropical cyclone Heat potential (TCHP). This NEMO global ocean data assimilation system is implemented at NCMRWF and generated ocean initial condition daily (Momin et al., 2020). The TCHP is computed by adding the heat content in a vertical column from sea surface to the 26°C isotherm depth.

$$TCHP = \rho C_p \int_0^{D20} (T - 26)dz$$

where, ρ is the density of the water and is derived from the ocean analysis of temperature, salinity and pressure. C_p is specific heat capacity of the sea water at constant pressure. T is the temperature of each layer. Figure 31 shows the TCHP (KJ/cm^2) from NEMO global ocean analysis during cyclone Amphan (12-20 May 2020) along with the IMD observed track. The high TCHP of more than 80 KJ/cm^2 is observed at 18°N (northern BoB region) from 12 May 2020 onward. This is the region where the strong warm core eddy (positive SLA) is observed (Figure 1(e)-(g)). This high TCHP is persists throughout the cyclone periods. However, the coastal BoB remains warm with TCHP more than 80 KJ/cm^2 throughout periods.

12. Summary and Conclusions

1) Prior to the development of cyclone Amphan over Bay of Bengal i.e., on 15th May 2020, the observed SSTs were warm and extended over entire BoB. During this time, the combined influence of low vertical shear and warm SST anomalies induces a favourable environment for the enhancement and sustainment of the cyclone. MSLP and associated surface winds also exhibits cyclonic circulation and low pressure. It is observed that the cyclone went into rapid intensification on 17th May 2020. DWR observations from Kolkata radar indicate the presence of large convective rainbands and large winds over west Bengal regions.
2) It is seen that NCUM global and regional products represent the well-marked low-pressure system and its intensification fairly well, during the course of the cyclonic storm. A close match in the movement, landfall and of the system is seen in both the analysis. On the other hand, the regional model forecasts slightly overestimate the intensity at all the forecast times. Further, the

center of the cyclone is slightly south eastward compared to the respective analysis and the IMD best track position.

3) The mean (all models) initial position errors is 48 km with highest error of 53 km in NCUM-R. Further, the mean (all models) 24-hour track errors are in the range of 54 km with highest error of 78 km in NCUM-R. Similarly, the mean track error at 48 and 72 hr is 114 km and 177 km respectively. NEPS-G has highest error of 133 km and 197 km at 48 and 72 hr lead time respectively.
4) The forecast track errors (DPE) computed for before naming of the cyclone (13-15 May 2020) are much smaller than compared to that after the naming of cyclone (16-21 May 2020). Before naming of cyclone the DPE for 48 h (*72h*) forecasts range from 85-93 km (*106-140 km*) and after the naming of the cyclone DPE for 48h (*72h*) forecasts range from 102-157 km (*169-272 km*).
5) Landfall position errors are lower than 50 km in all forecasts from 12 UTC 18th May2020 (except the forecast based on 00 UTC 19th May 2020 when landfall position error was over 80 km). Forecast landfall time error is mostly early (-ve). Highest error of -11 hours is seen in NCUM-G forecast based on 00 UTC 16th May 2020. All forecasts made after 00 UTC 18th May2020 have relatively low time errors ranging from -03:30h to +01:30h.
6) Forecasts show delayed peak intensity in NCUM-G and NEPS-G by over 1 day. The 24, 48, and 72 hr errors in forecast MSLP range from 10-15, 11-17 and 15-24 hPa respectively. Similarly, the 24, 48 and 72 hr errors in forecast Maximum Winds range from 18-20, 16-19 and 14-19 kt respectively.
7) The ensemble-based strike probability forecasts verified using the reliability and ROC show marginally improved performance in the experimental (23-member) compared to the operational (12-member).
8) MJO influence during the cyclone Amphan shows that the dominant intraseasonal signal is acting during 15-20 May 2020. The enhanced active phase of MJO as seen in NEPS-G forecasts is favouring the sustainment of cyclone.
9) NEMO Coupled model analysis shows that the omnipresence of large TCHP (>80 KJ/cm^2) values over BoB region enhanced the strength of the cyclone.

References

1. Bullock, R. G., Brown, B. G., & Fowler, T. L., 2016: Method for Object-Based Diagnostic Evaluation (No. NCAR/TN-532+STR). https://doi.org/:10.5065/D61V5CBS.

2. Ebert, E. E and J. L. McBride, 2000: Verification of Precipitation in weather systems: Determination of systematic errors. *J. Hydrology, 239*, 179-202.

3. Ebert, E. E and W. A. Gallus, 2009: Toward better understanding of the contiguous rain area (CRA) verification method. *Weather Forecasting, 24*, 1401-1415.

4. Heming, J. T., 2017: Tropical cyclone tracking and verification techniques for Met Office numerical weather prediction models. *Meteorol. Appl., 24 (1)*, 1-8.

5. Kuldeep Sharma, R. Ashrit, E. Ebert, A. K. Mitra, R. Bhatla, Gopal Iyengar and E. N. Rajagopal, 2019: Assessment of Met Office Unified Model (UM) quantitative precipitation forecasts during the Indian Summer Monsoon: Contiguous Rain Area (CRA) Approach. Journal of Earth System Sciences,128(4), https://doi.org/10.1007/s12040-018-1023-3
6. Mitra A. K., A. K. Bohra, M. N. Rajeevan and T. N. Krishnamurti, 2009. Daily Indian precipitation analysis formed from a merge of rain-gauge data with the TRMM TMPA satellite-derived rainfall estimates. J. Meteorol. Soc. Japan. 87A, 265-279.

7. Momin I. M., Ashis K. Mitra and E. N. Rajagopal, 2020: Implementation of NEMO based Global 3D-Var Ocean Data Assimilation System at NCMRWF: Technical Aspects, *NMRF/TR/02/2020*, 26p.
8. Saffir H. S., 1973: Hurricane wind and storm surge. *Mil. Eng., 423*, 4–5.
9. Shay L. K., G. J. Goni and P. G. Black, 2000: Effect of a warm ocean ring on hurricane Opal. *Mon. Wea. Rev.*, 128, 1366-1383. https://doi.org/10.1175/1520-0493(2000)128<1366:EOAWOF>2.0.CO;2.
10. Simpson R. H., 1974: The hurricane disaster potential scale. *Weatherwise, 27*, 169, 186.

11. Wheeler, M. C., and H. H. Hendon, 2004: An All-Season Real-Time Multivariate MJO Index: Development of an Index for Monitoring and Prediction. *Mon. Wea. Rev.*, **132**, 1917–1932, https://doi.org/10.1175/1520-0493(2004)132<1917:AARMMI>2.0.CO;2.

12. Sumit Kumar, A. Jayakumar, M. T. Bushair, Buddhi Prakash J., Gibies George, Abhishek Lodh, S. Indira Rani, Saji Mohandas, John P. George and E. N. Rajagopal, 2018: Implementation of New High Resolution NCUM Analysis-Forecast System in Mihir HPCS, NMRF/TR/01/2018, 17p. (https://www.ncmrwf.gov.in/NCUM-Report-Aug2018_final.pdf).

Appendix -I

Table 1: NCMRWF Unified Model configuration since June 2018

Model	Application & Domain	Resolution	Forecasts
NCUM-G	Global Deterministic Model	N1024L70 (12 km horizontal resolution with 70 vertical levels)	00 UTC: Day 1 to Day 10 12 UTC: Day 1 to Day 10
NEPS-G	Global Ensemble Model	N1024L70 (12 km horizontal resolution; Control+ 22 member)	00 UTC: Day 1 to Day 10 12 UTC: Day 1 to Day 10
NCUM-R	Regional Deterministic Model high resolution over Indian region (5-40°N and 65-100°E)	4 km resolution Explicit convection	00 UTC: Day 1 to Day 3 12 UTC: Day 1 to Day 3
NEPS-R	Regional Ensemble Model high resolution over Indian region (7-38°N and 67-98°E)	4 km resolution (Control+ 11 members) Explicit convection	00 UTC: Day0 to Day3

Table 2: Forecast Track Errors for SCS Amphan from 13-21 May2020. NCUM-G, NEPS-G and NCUM-R track errors are based on 00 UTC and 12 UTC (numbers in the brackets indicate number of cases)

Forecast Hour	0	24	48	72	96	120
NUCM-G	43 (10)	68 (12)	112 (12)	183 (11)	210 (10)	250 (8)
NEPS-G	53 (11)	68 (12)	133 (12)	197 (11)	229 (9)	190 (7)
NCUM-R	48 (11)	78 (12)	99 (12)	153 (11)		

Table 3: Forecast track errors before the naming of the cyclone (13-15 May 2020) and after the naming of cyclone (16-21 May2020)

Forecasts based on 13-21 May 2020											
Forecast Hour	**0**	**12**	**24**	**36**	**48**	**60**	**72**	**84**	**96**	**108**	**120**
NCUM-G	43	65	68	94	112	148	183	205	210	227	250
NEPS-G	53	61	68	101	133	173	197	223	229	209	190
NCUM-R	48	72	78	86	99	118	153				
Forecasts based on 13-15 May 2020											
NCUM-G		144	94	70	86	81	140	146	139	159	171
NEPS-G		88	20	57	85	95	106	126	145	155	154
NCUM-R		80	63	59	93	103	138				
Forecasts based on 16-21May 2020											
NCUM-G	43	58	62	98	124	187	237	294	326	429	
NEPS-G	53	58	77	117	157	219	272	321	335	310	282
NCUM-R	48	71	81	95	102	131	169				

Table 4: Error in the forecast landfall time and position
(Forecast time – Observed time) **[-*ve*=*early* +*ve*=*delay*]**

	NCUM-G		**NEPS-G**		**NCUM-R**	
Initial Condition (IC)	**Time error (hr:min)**	**Position error (km)**	**Time-error (hr:min)**	**Position error (km)**	**Time-error (hr:min)**	**Position error (km)**
00 UTC 16052020	-11:00	263	-09:00	268		
12 UTC 16052020	-07:30	200	-07:00	180		
00 UTC 17052020	-04:00	105	-07:00	198		
12 UTC 17052020	-03:30	200	-01:30	155	-04:00	145
00 UTC 18052020	01:00	143	-00:30	165	-00:30	57
12 UTC 18052020	-03:30	23	-02:00	26	-00:30	26
00 UTC 19052020	-02:00	37	-03:00	84	0:00:	0
12 UTC 19052020	-01:00	12	-00:30	12	0:00:	12
00 UTC 20052020	-00:30	8	-01:30	12	1:30:	5

Appendix –II

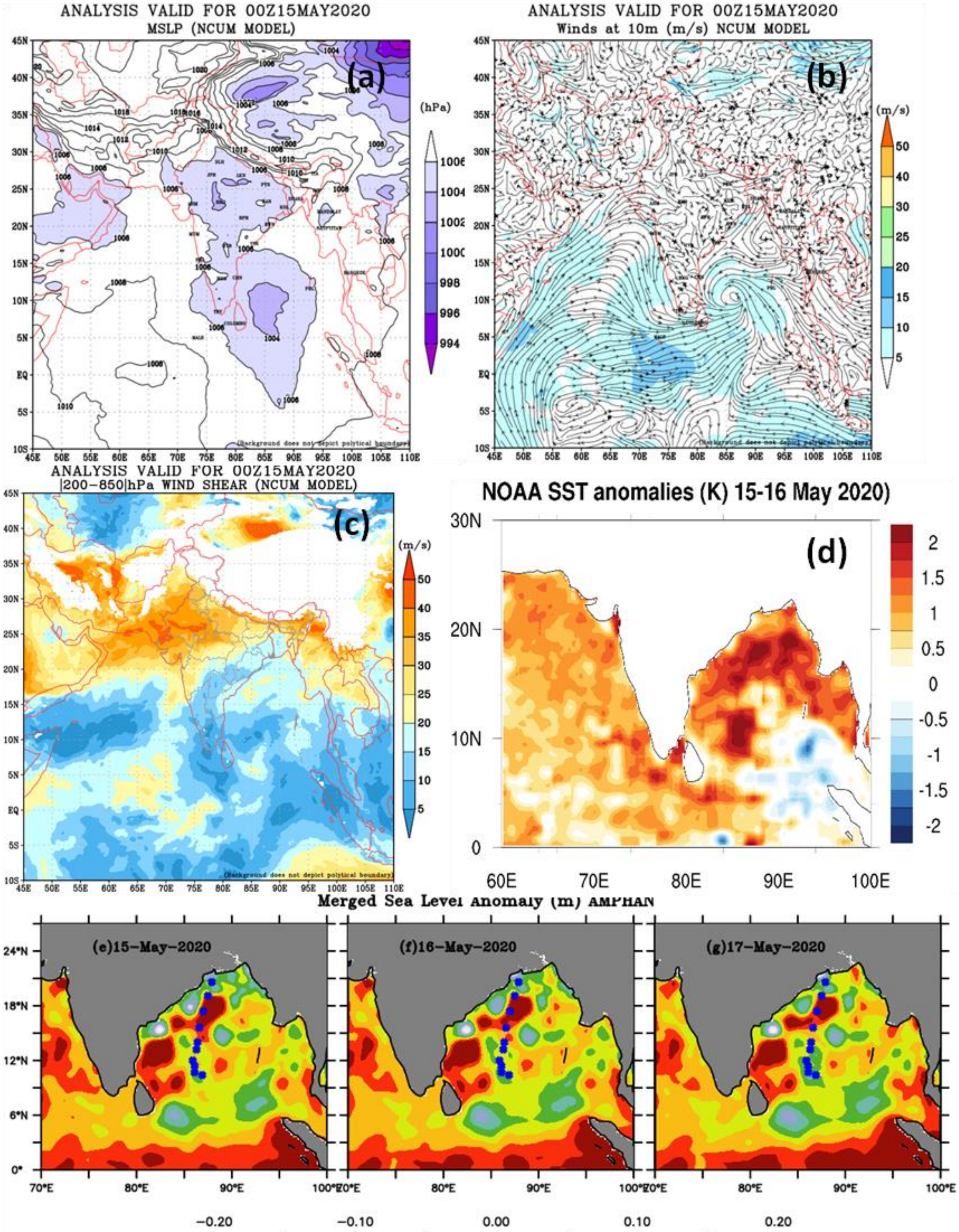

Figure 1: NCUM global analysis of (a) mean sea level pressure (MSLP); (b) winds at 10m; (c) low-vertical shear (200-850 hPa) and (d) NOAA interpolated SST (K) anomalies during 15-16 May 2020 and (e)-(g) shows the observed sea level anomaly (SLA) during 15-17 May 2020. Blue dotted line shows the IMD best track

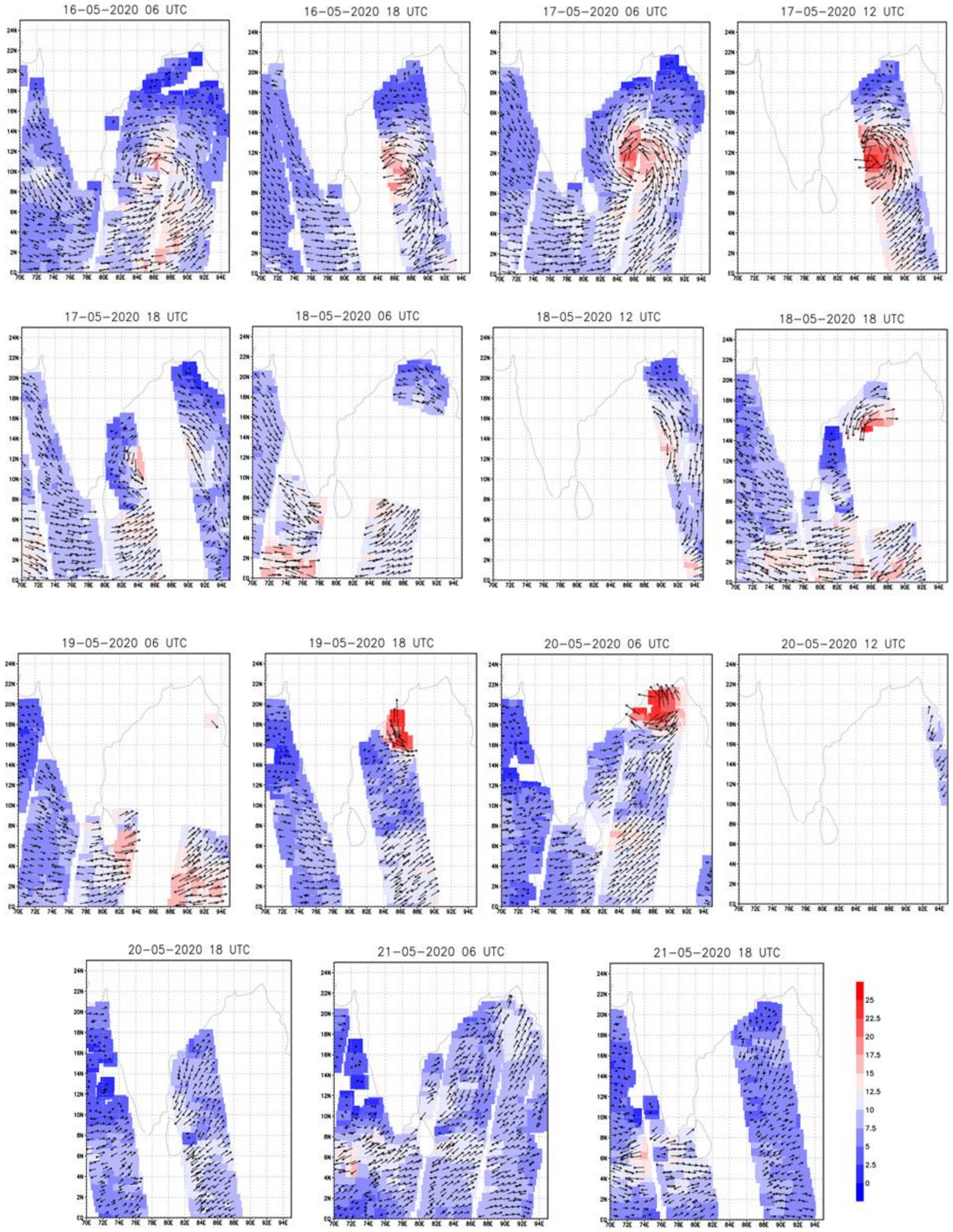

Figure 2: Scatterometer winds assimilated during the period of cyclone Amphan. In the figure wind vectors are shown in black arrows and the shading indicates the wind speed in m/s

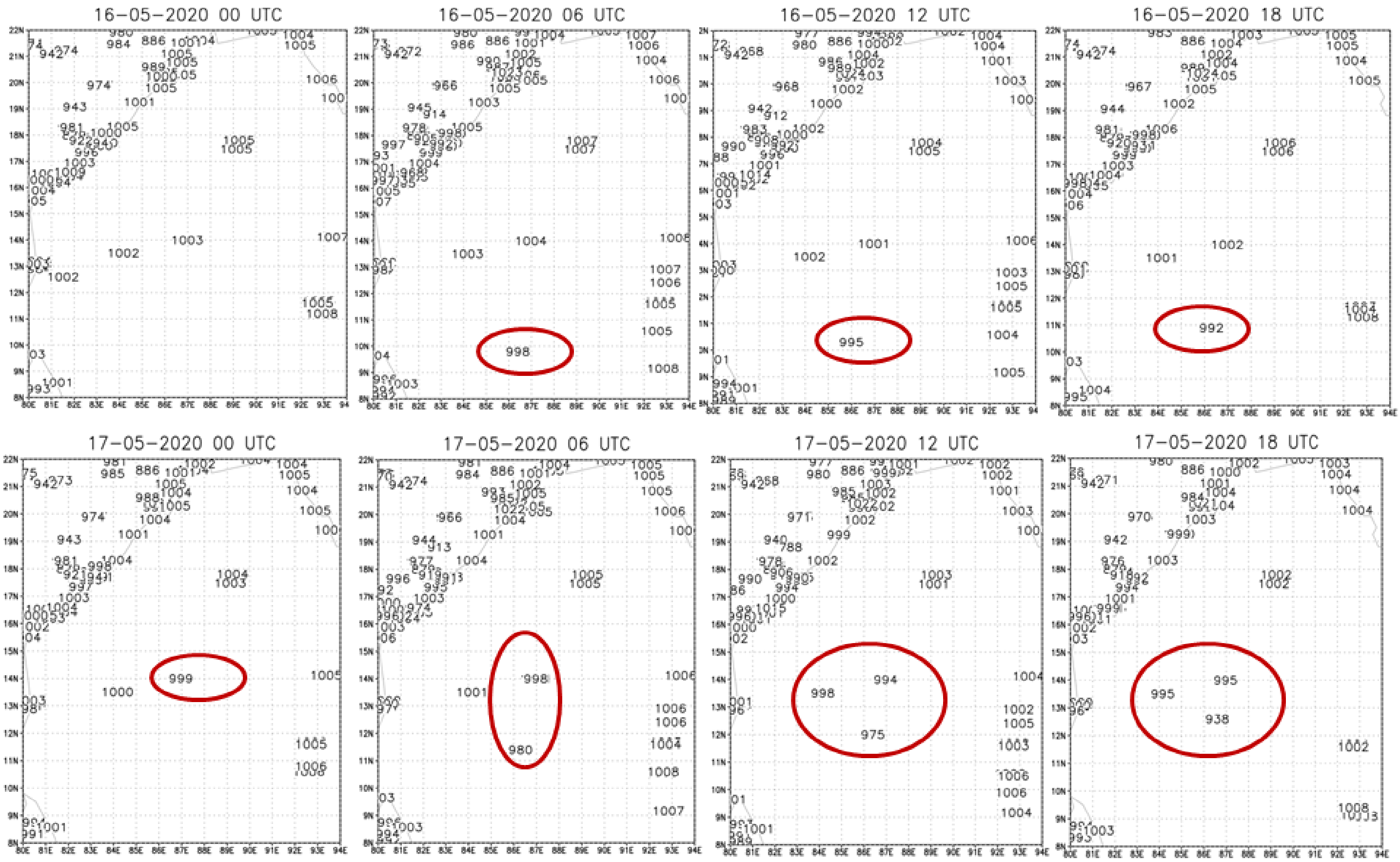

Figure 3: Surface observations over the Ocean (Buoy pressure) assimilated during the period of Amphan cyclone. Each row represents the four assimilation cycles on 16 & 17 May 2020

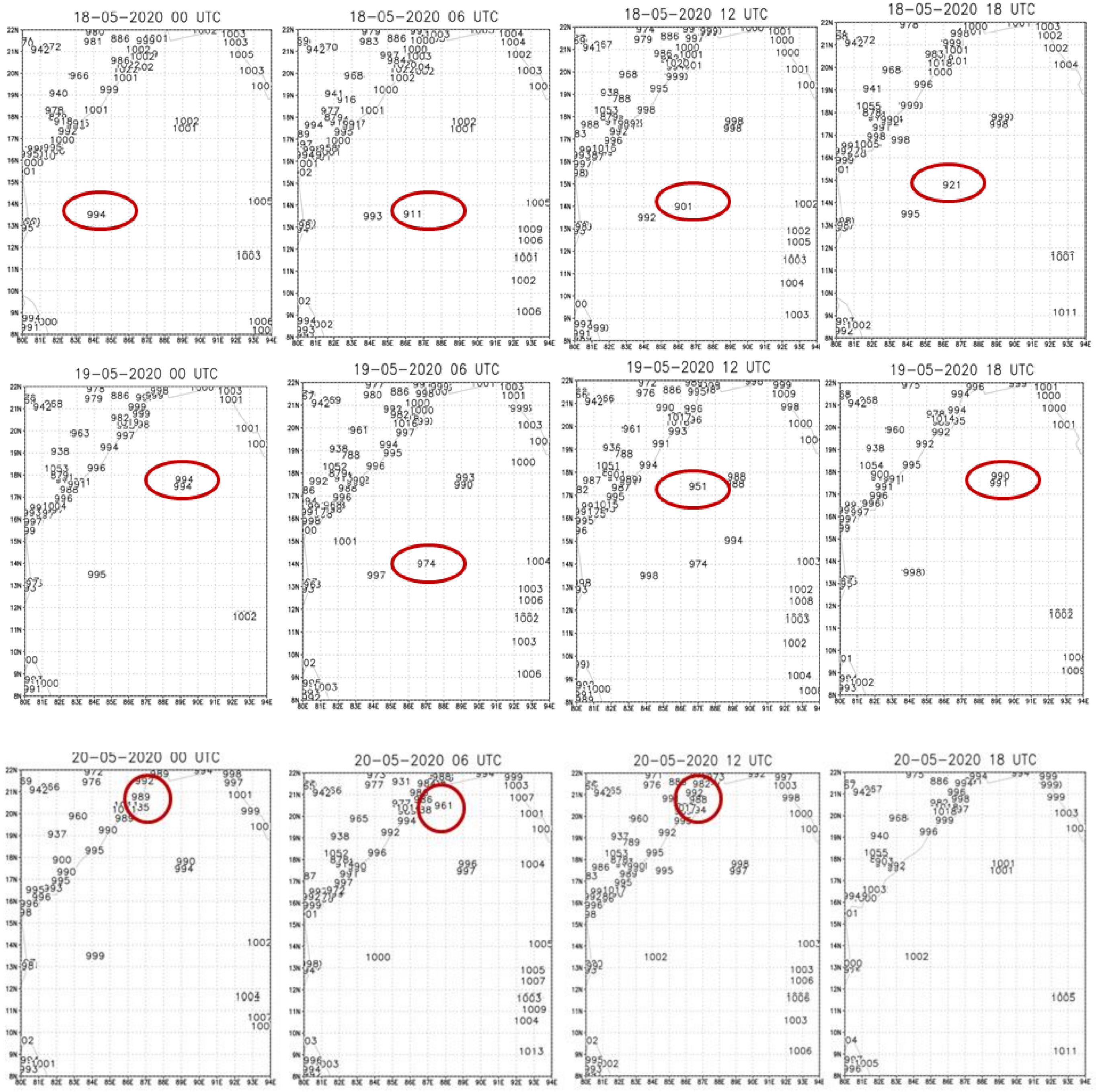

Figure 4: Surface observations over the Ocean (Buoy pressure) assimilated during the period of Amphan cyclone. Each row represents the four assimilation cycles from 18 to 20 May 2020

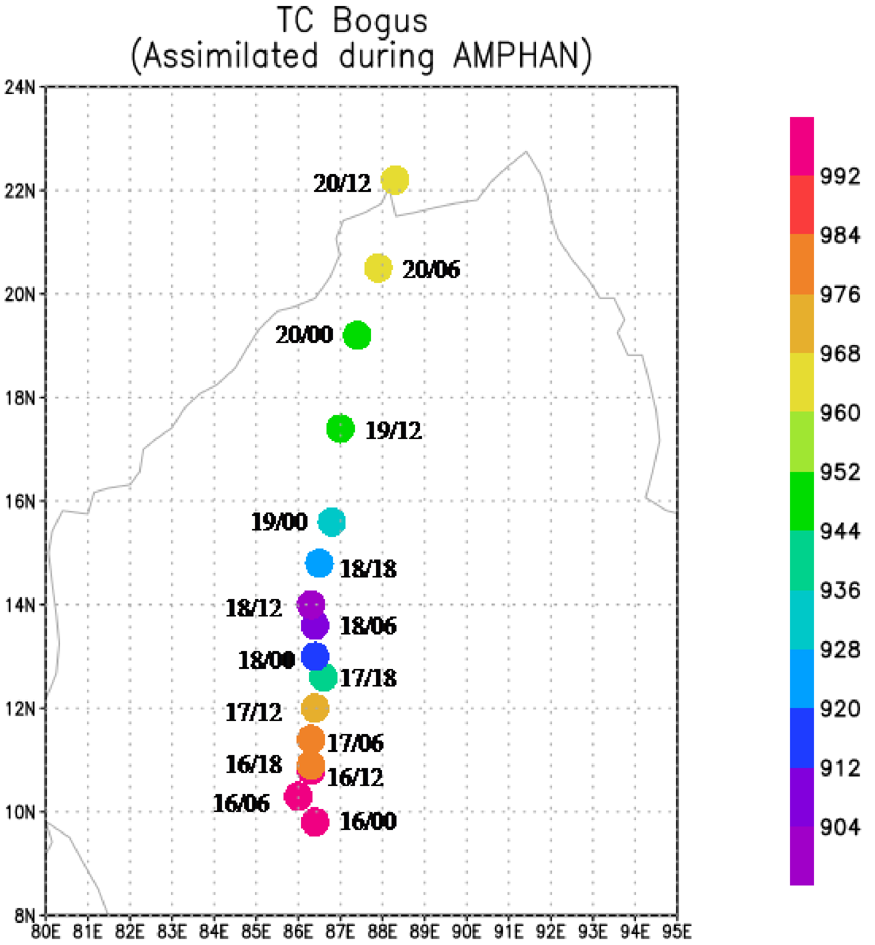

Figure 5: Location of pressure from TC-Vitals assimilated in the NCUM-G during AMPHAN cyclone (denoted the time next to the observation)

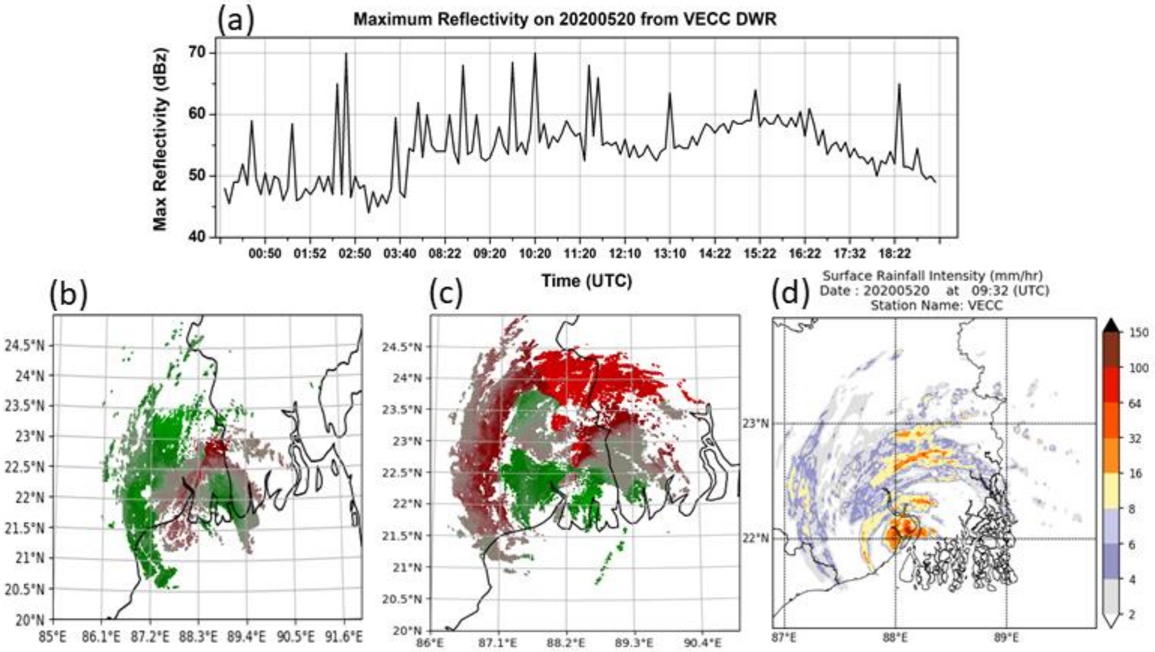

Figure 6: (a) Temporal evolution of maximum reflectivity seen by Kolkata DWR on 20th May 2020; (b) and (c) radial velocity seen Kolkata DWR before and after landfall at 08:10 and 10:50 UTC, respectively; (d) Instantaneous surface rainfall intensity computed by Kolkata DWR at 09:32 UTC

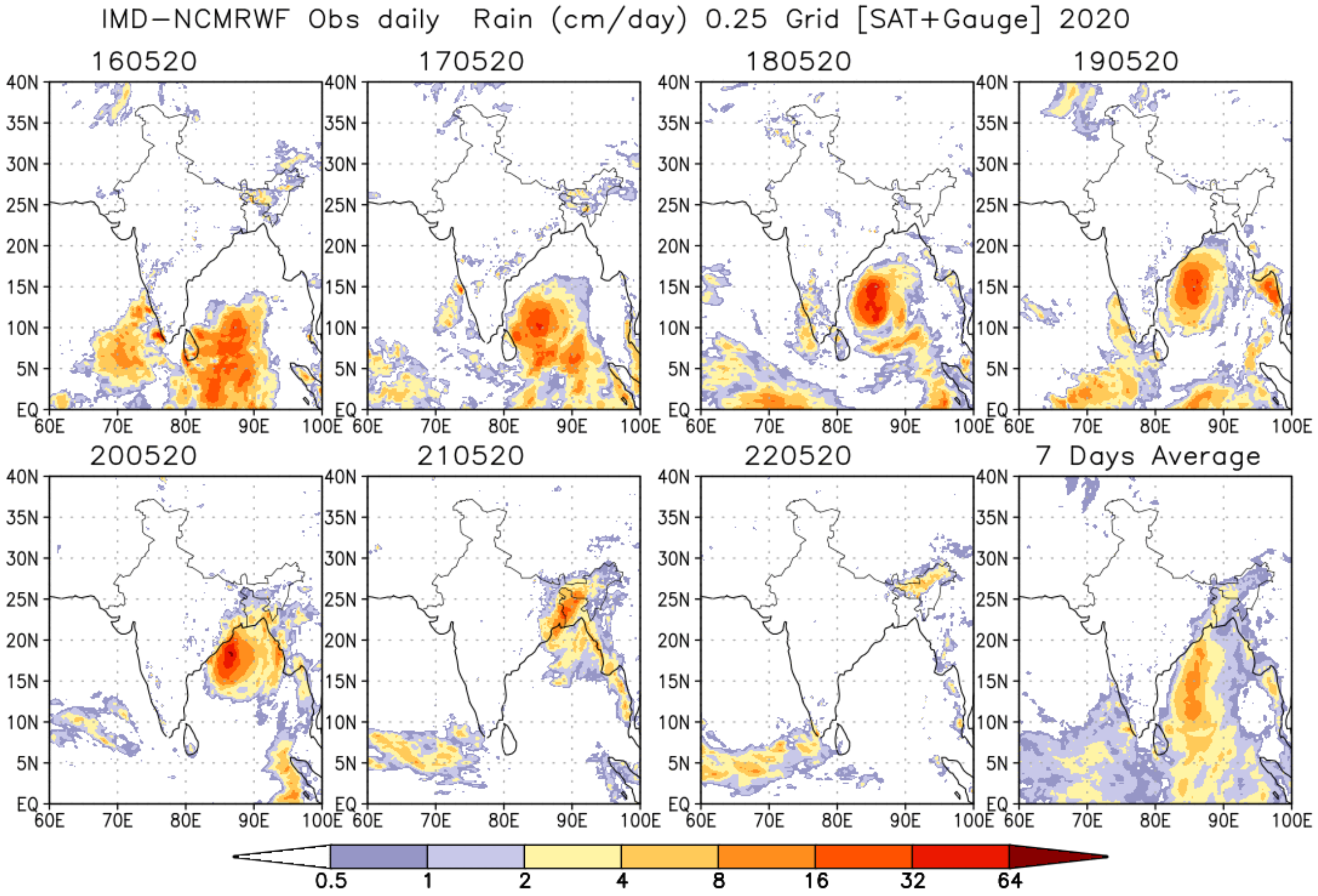

Figure 7: Space-time evolution of observed merged (satellite + gauge) gridded rainfall product during the Amphan evolution from 16-22 May 2020. The last panel plot shows the 7 day average rainfall. Units of rainfall in cm/day

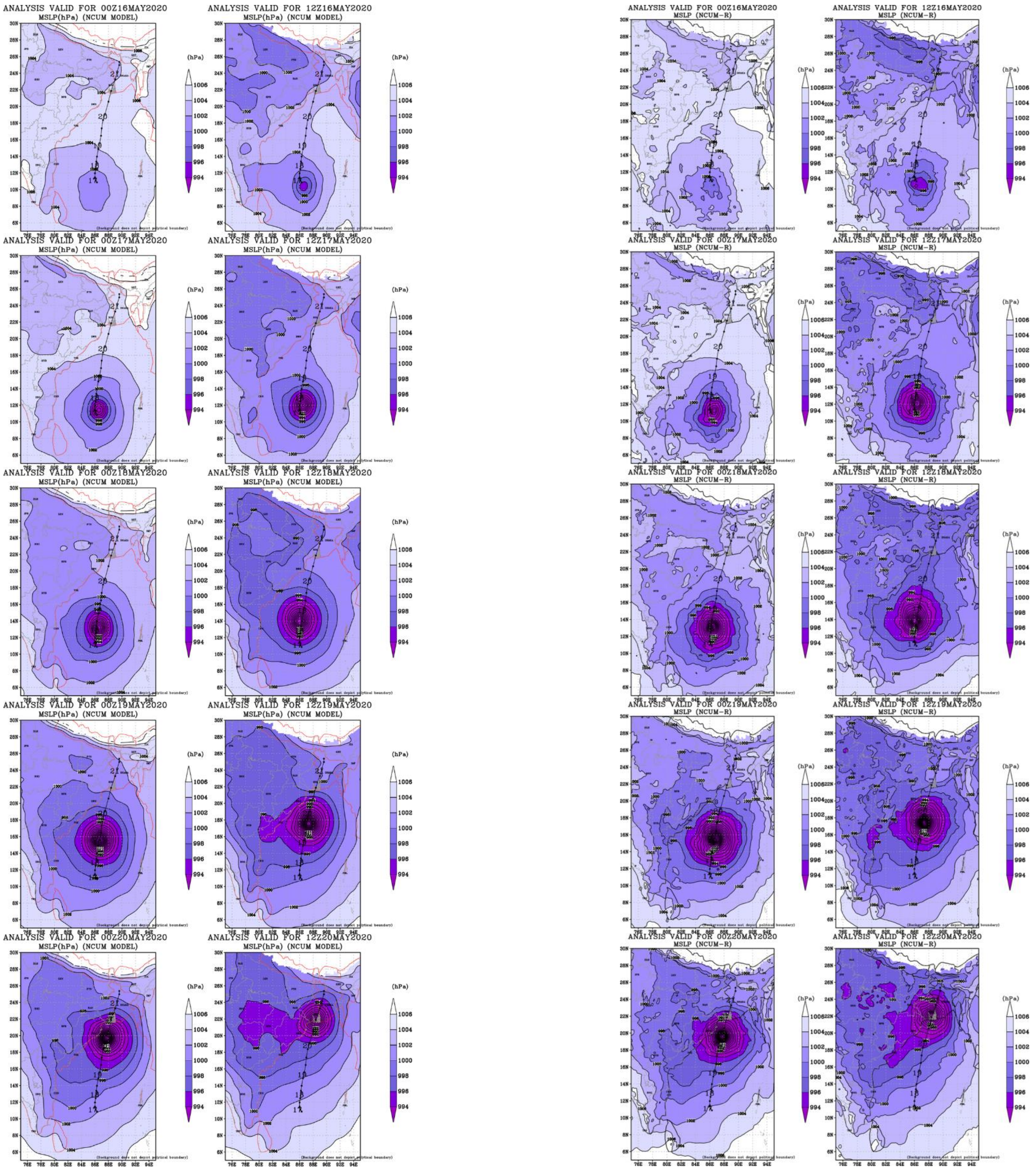

Figure 8: NCUM-G (left) and NCUM-R (right) MSLP analysis during 16-20 May 2020 for 00 and 12 UTC

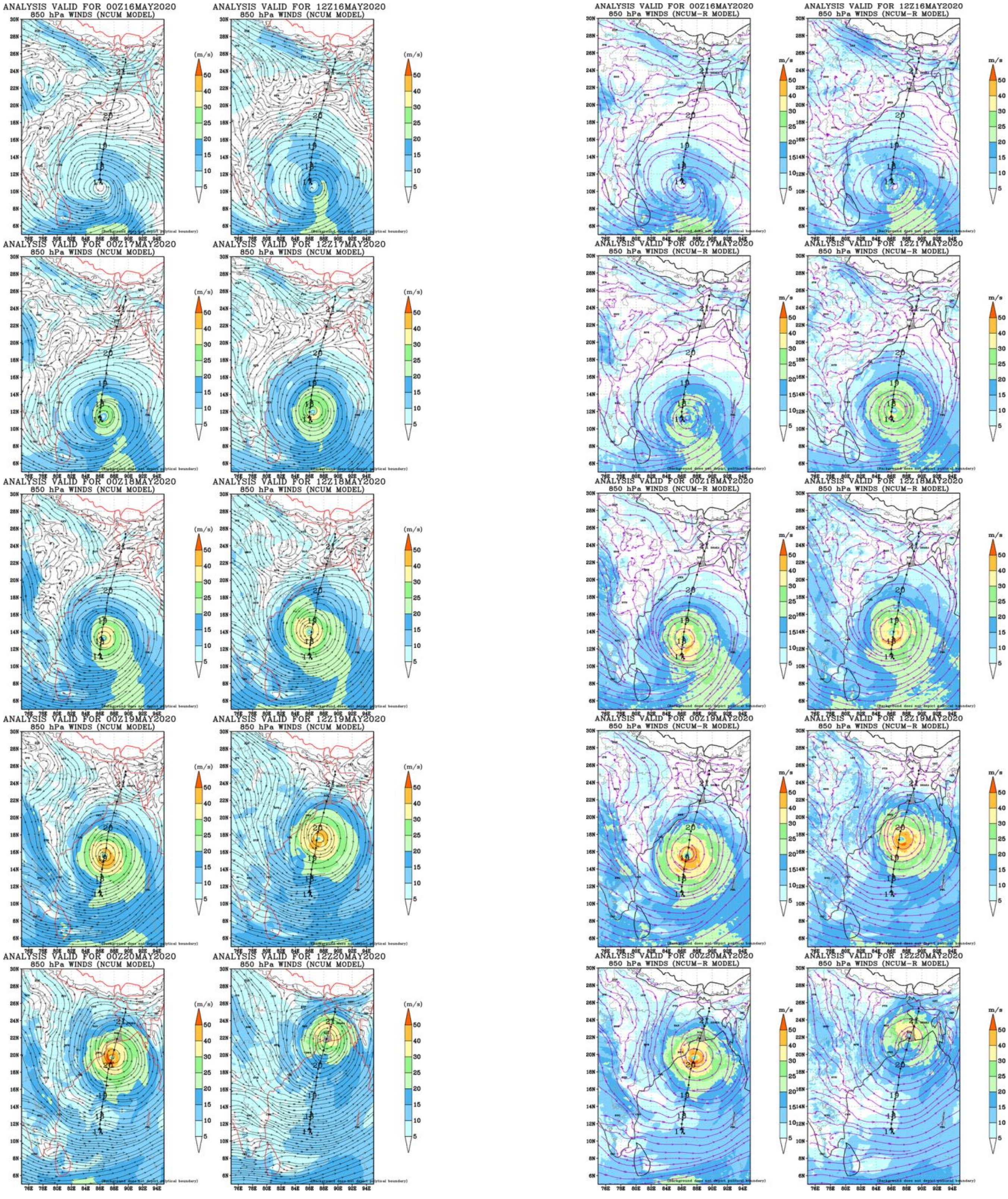

Figure 9: As in Figure 8 for 850 hPa Winds

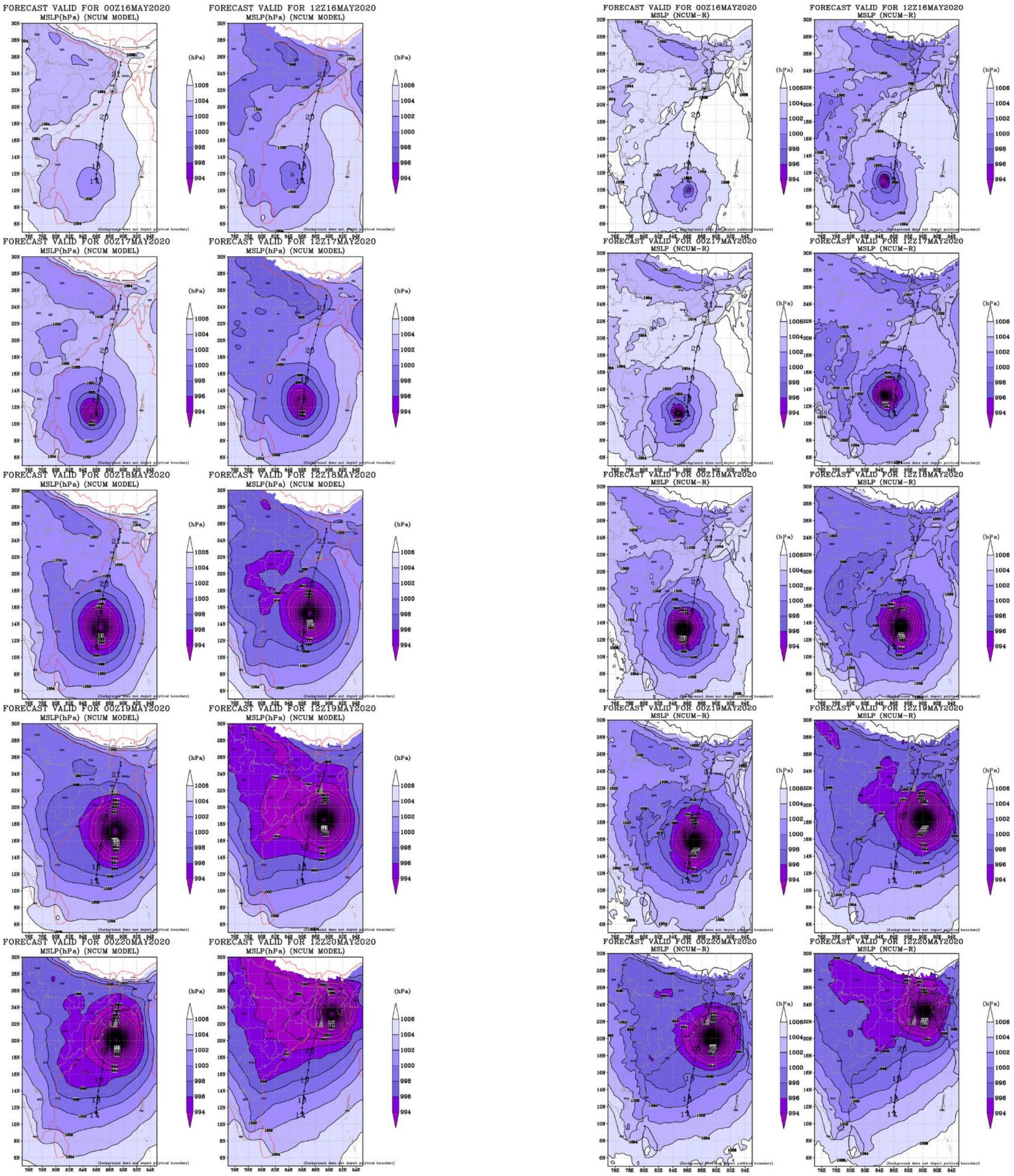

Figure 10: NCUM-G (left) and NCUM-R (right) Day-3 forecast MSLP during 16-20 May 2020 for 00 and 12 UTC

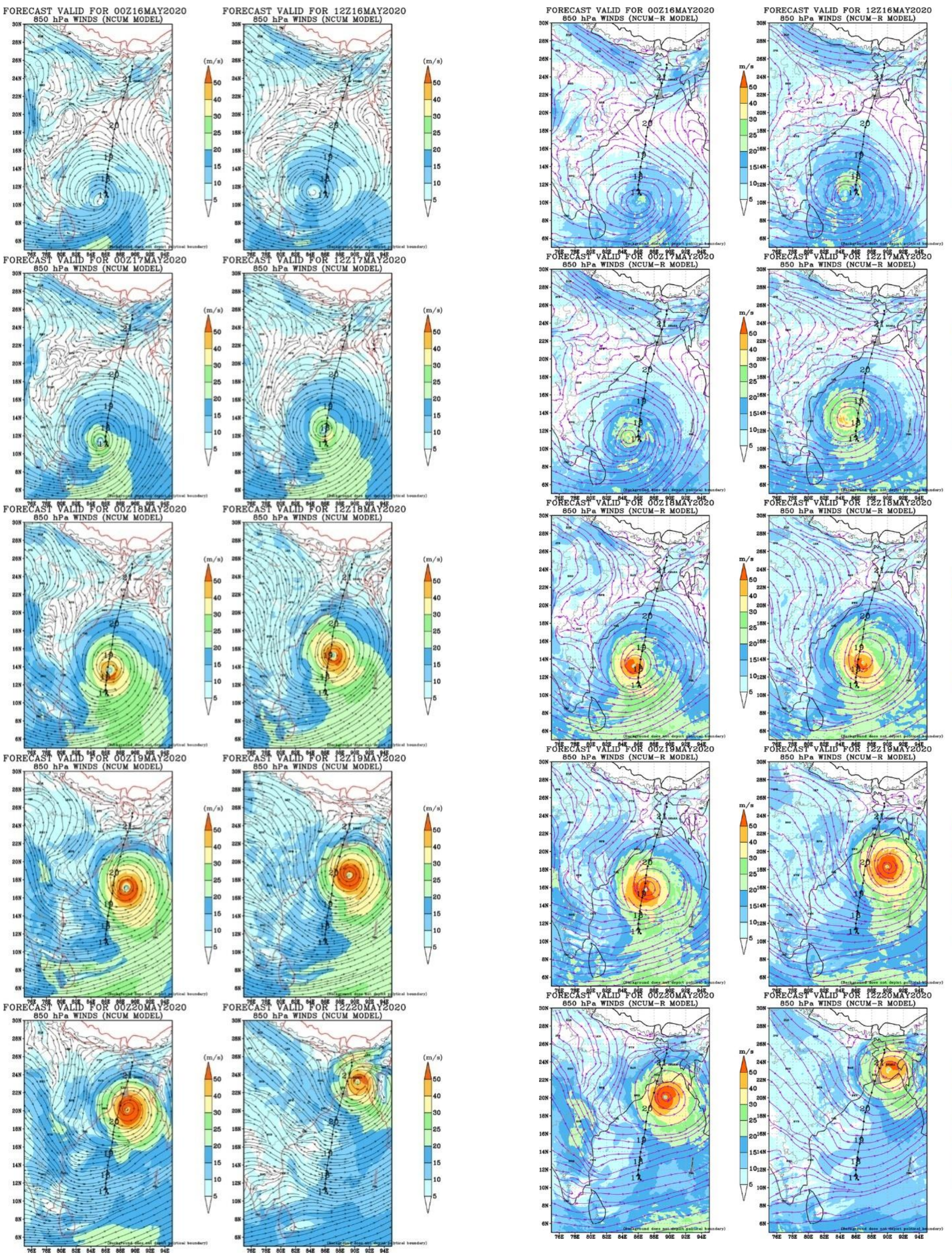

Figure 11: As in Figure 10 for 850 hPa Winds

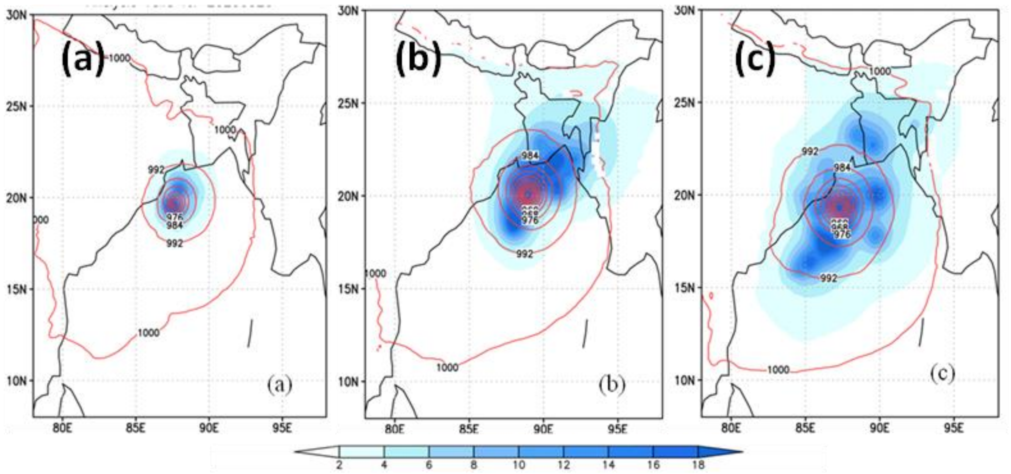

Figure 12: Ensemble (NEPS-G) mean (contour) and spread (shaded) in (a) Analysis, (b) Day-3 and (c) Day-5 forecast of MSLP valid for 00 UTC 20th May 2020

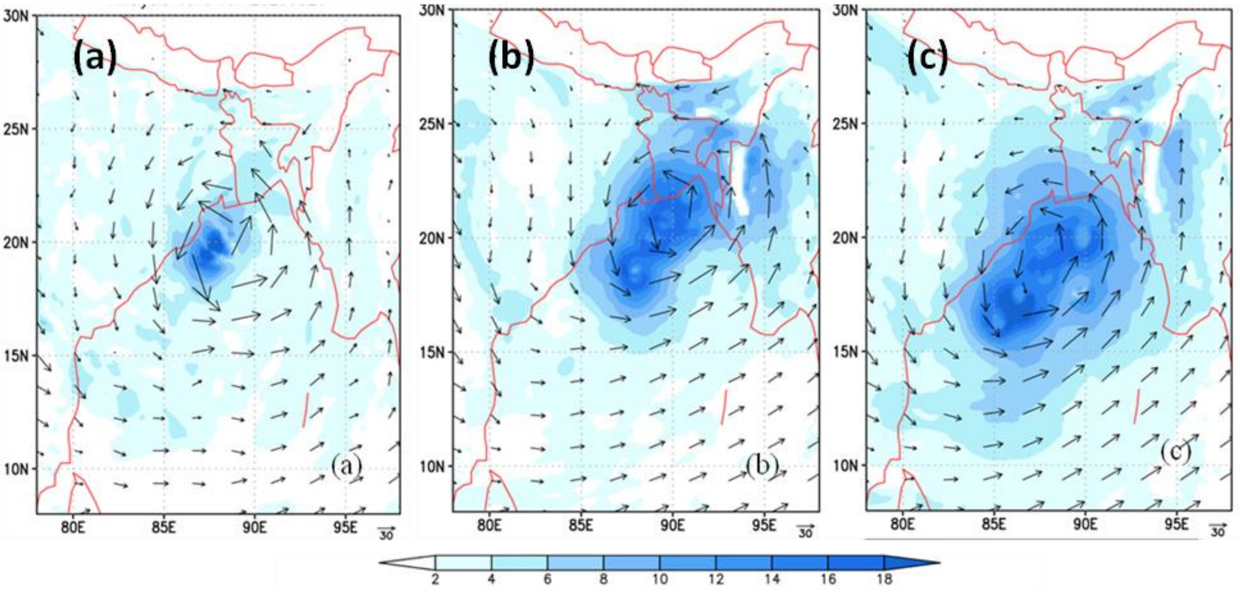

Figure 13: Ensemble (NEPS-G) (vector) and spread (shaded) in (a) Analysis, (b) Day-3 and (c) Day-5 forecast of wind at 850 hPa valid for 00 UTC 20th May 2020

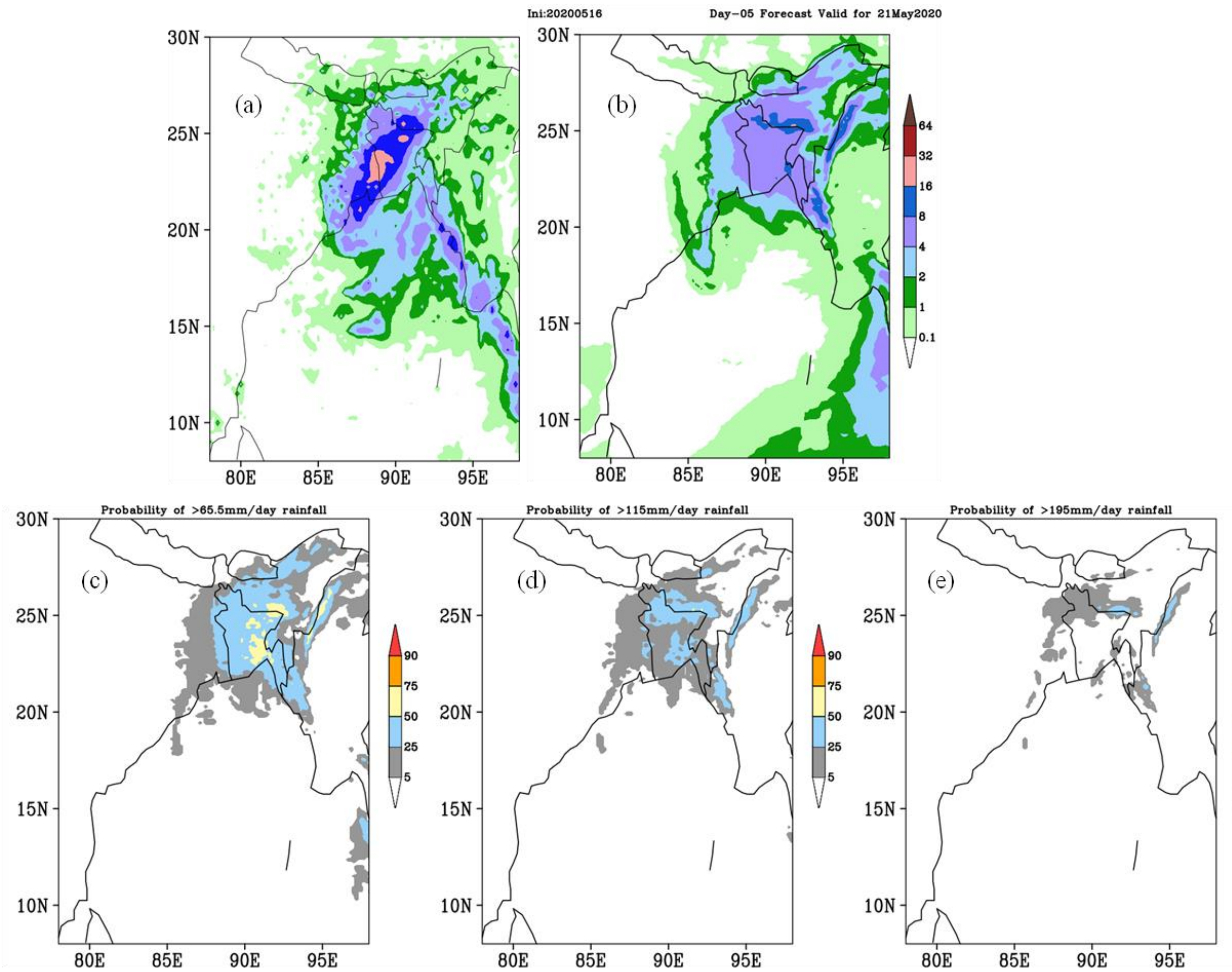

Figure 14: (a) Observed NSMG rainfall on 21st May 2020, NEPS-G Day-5 forecast of (b) Ensemble mean precipitation and Probabilistic quantitative precipitation forecast exceeding (c) 65.5, (d) 115 and (e) 195 mm/day valid for 00 UTC 21st May 2020

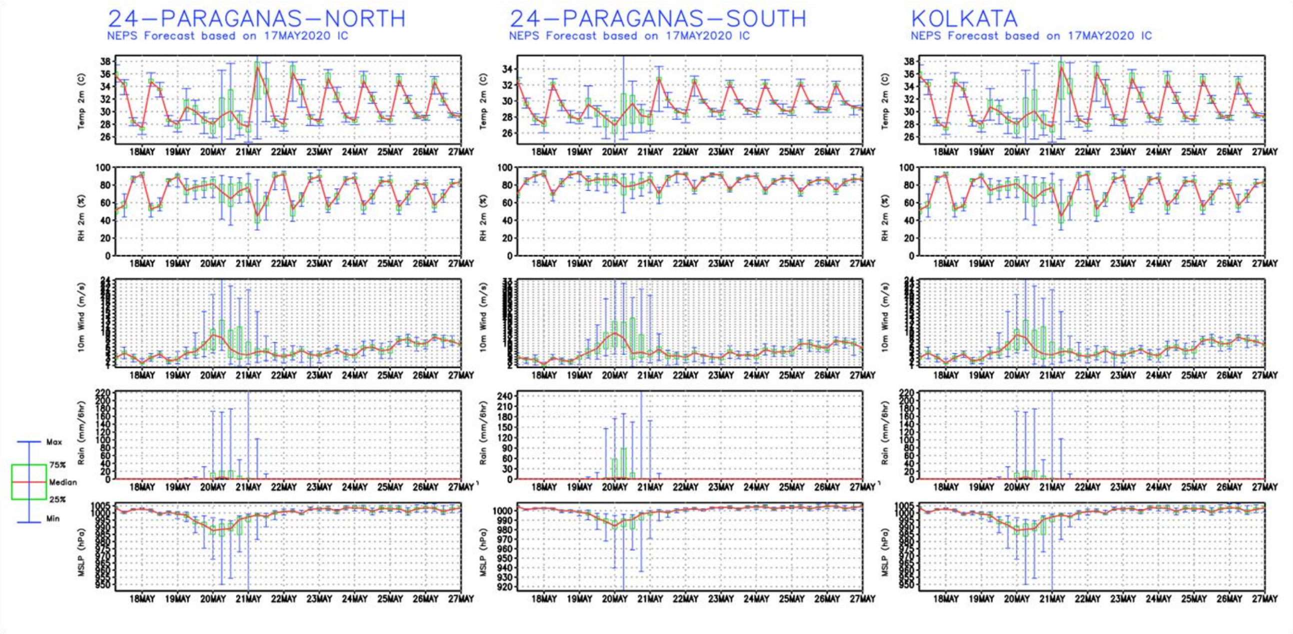

Figure 15: NEPS-G EPSGRAM for 24-Parganas North, South and Kolkata based on 17th May 2020 initial conditions, depicting Temperature (°C) & Relative Humidity at 2m (%), 10m wind (m/s), rainfall (mm/6hr) and MSLP (hPa) for next 10 days

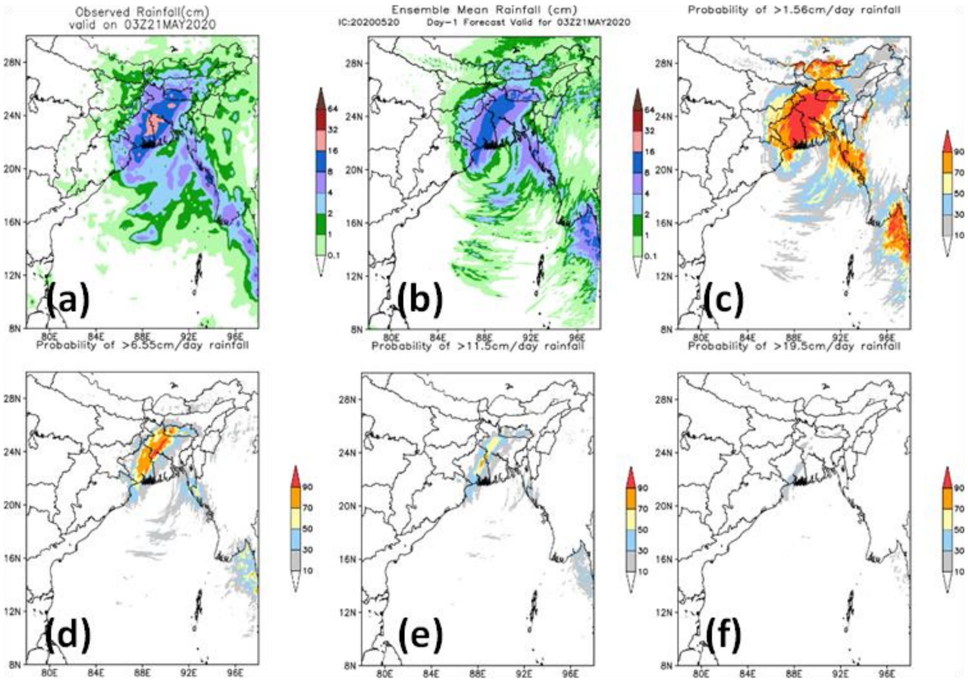

Figure 16: (a) Observed (satellite-gauge merged) rainfall (b) Ensemble mean rainfall (cm) forecast (Day-1) and probabilistic quantitative precipitation forecast of NEPS-R for Day-1, (c) >1.56 cm, (d) >6.55 cm, (e) >11.5 cm and (f) >19.5 cm valid for 03 UTC 21st May 2020

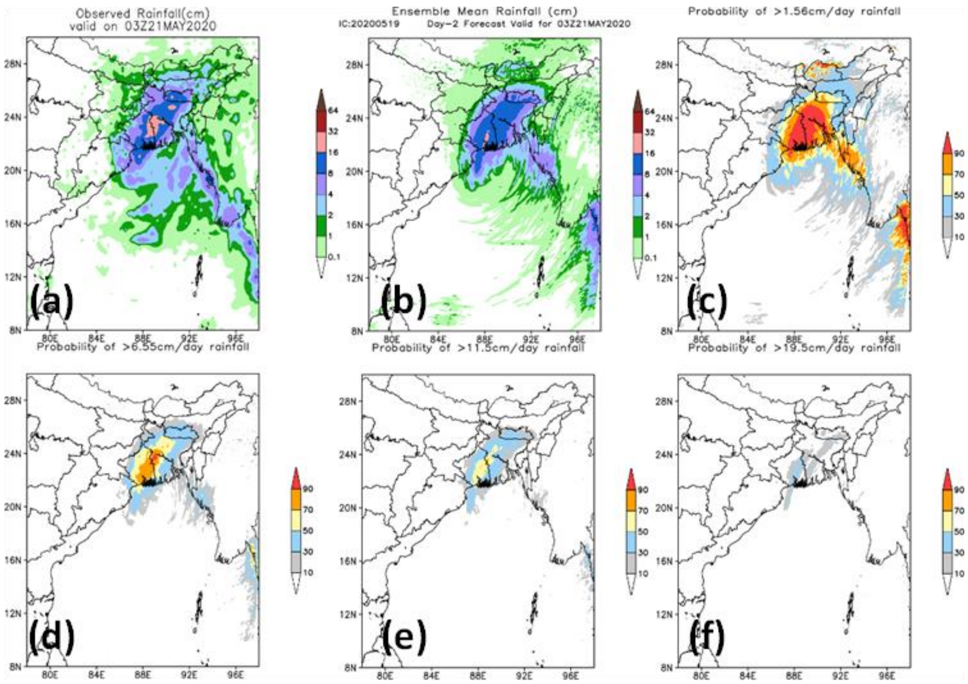

Figure 17: (a) Observed (satellite-gauge merged) rainfall (b) Ensemble mean rainfall (cm) forecast (Day-2) and probabilistic quantitative precipitation forecast of NEPS-R for Day-2, (c) >1.56 cm, (d) >6.55 cm, (e) >11.5 cm and (f) >19.5 cm valid for 03 UTC 21 May, 2020

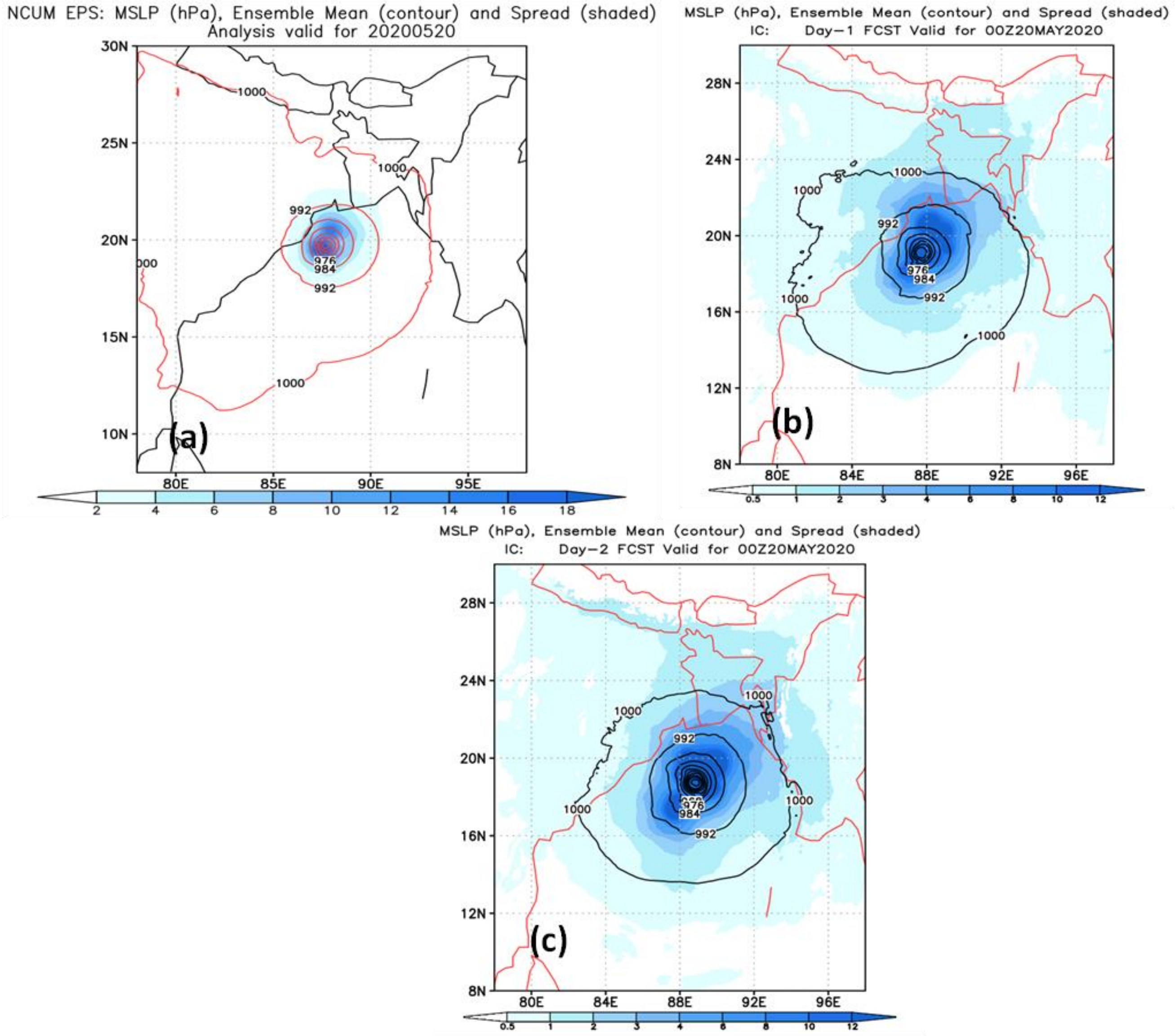

Figure 18: NEPS-R Ensemble mean (contour) and spread (shaded) in (a) Analysis, (b) Day-1 and (c) Day-2 forecast of MSLP valid for 00 UTC 20th May 2020.

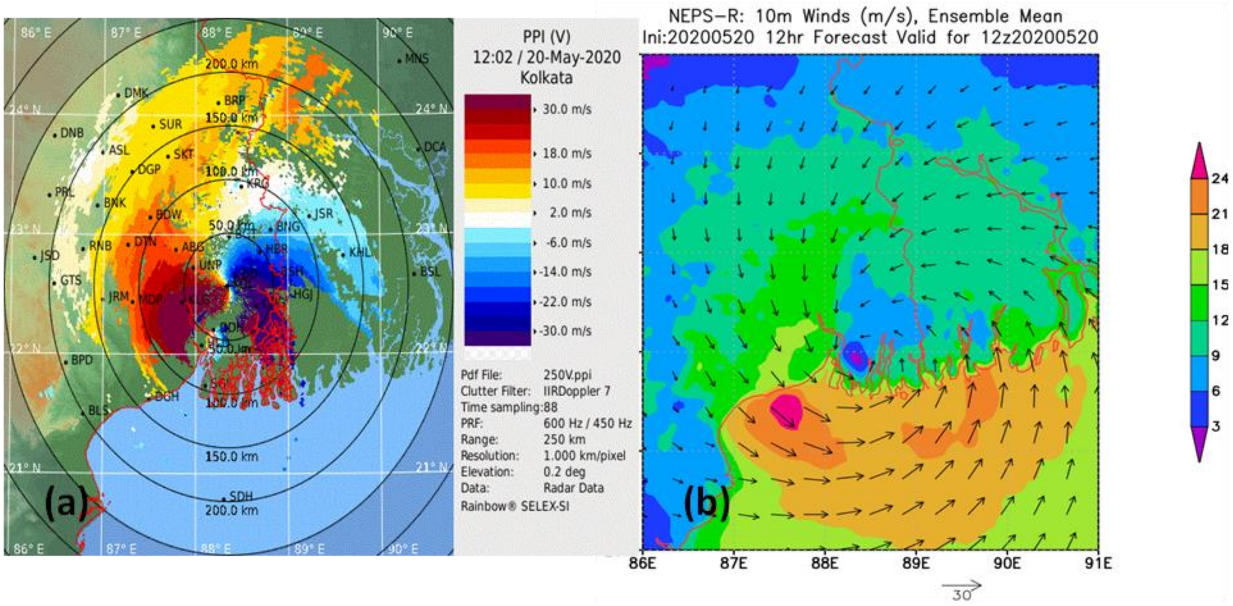

Figure 19: (a) Observed radar winds (b) NEPS-R ensemble mean forecast of 10m wind valid for 12 UTC 20th May 2020.

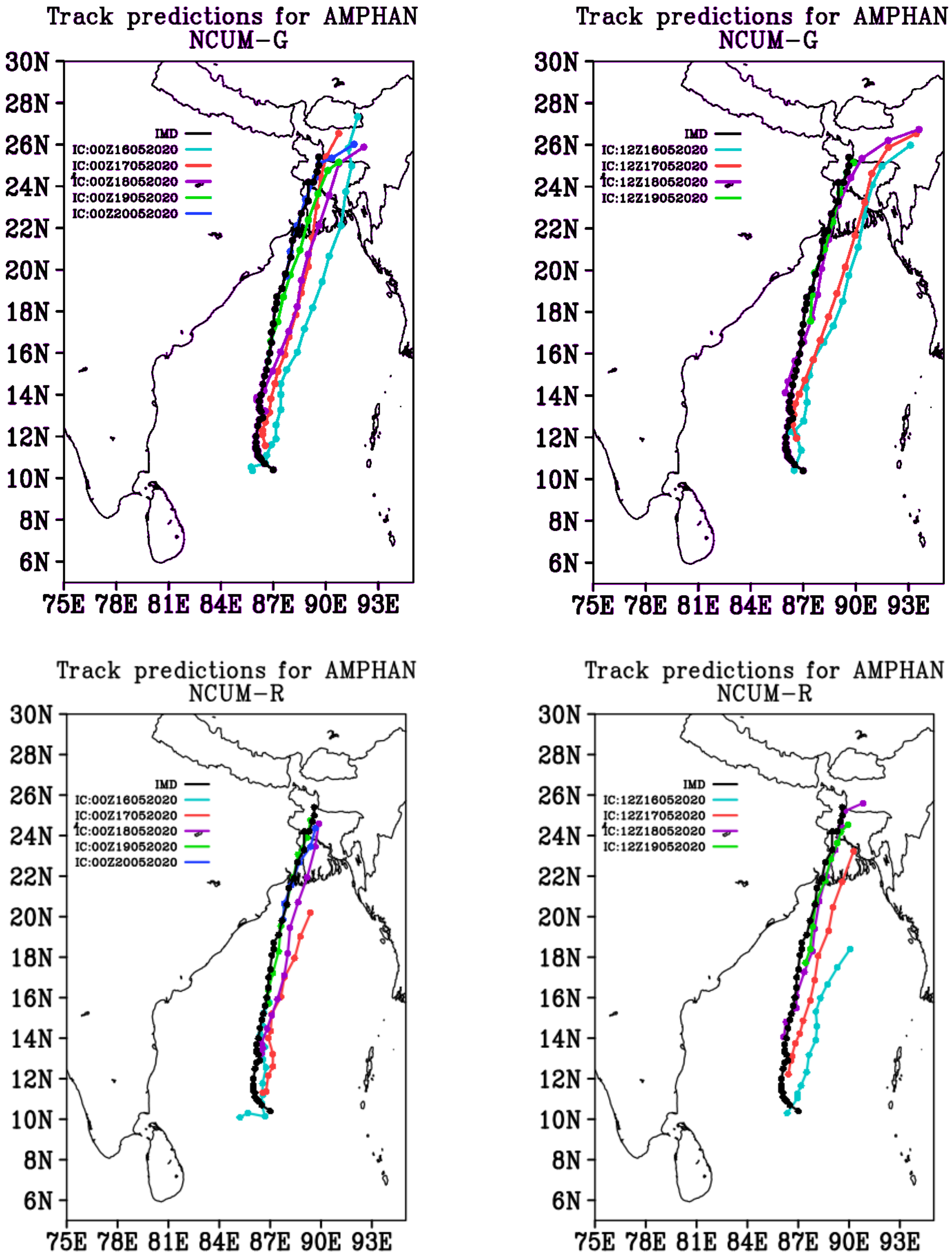

Figure 20: Observed and model forecast tracks for cyclone Amphan based on NCUM-G (top) and NCUM-R (bottom) are shown for 00UTC (left) and 12 UTC (right) forecasts during 16-20 May 2020.

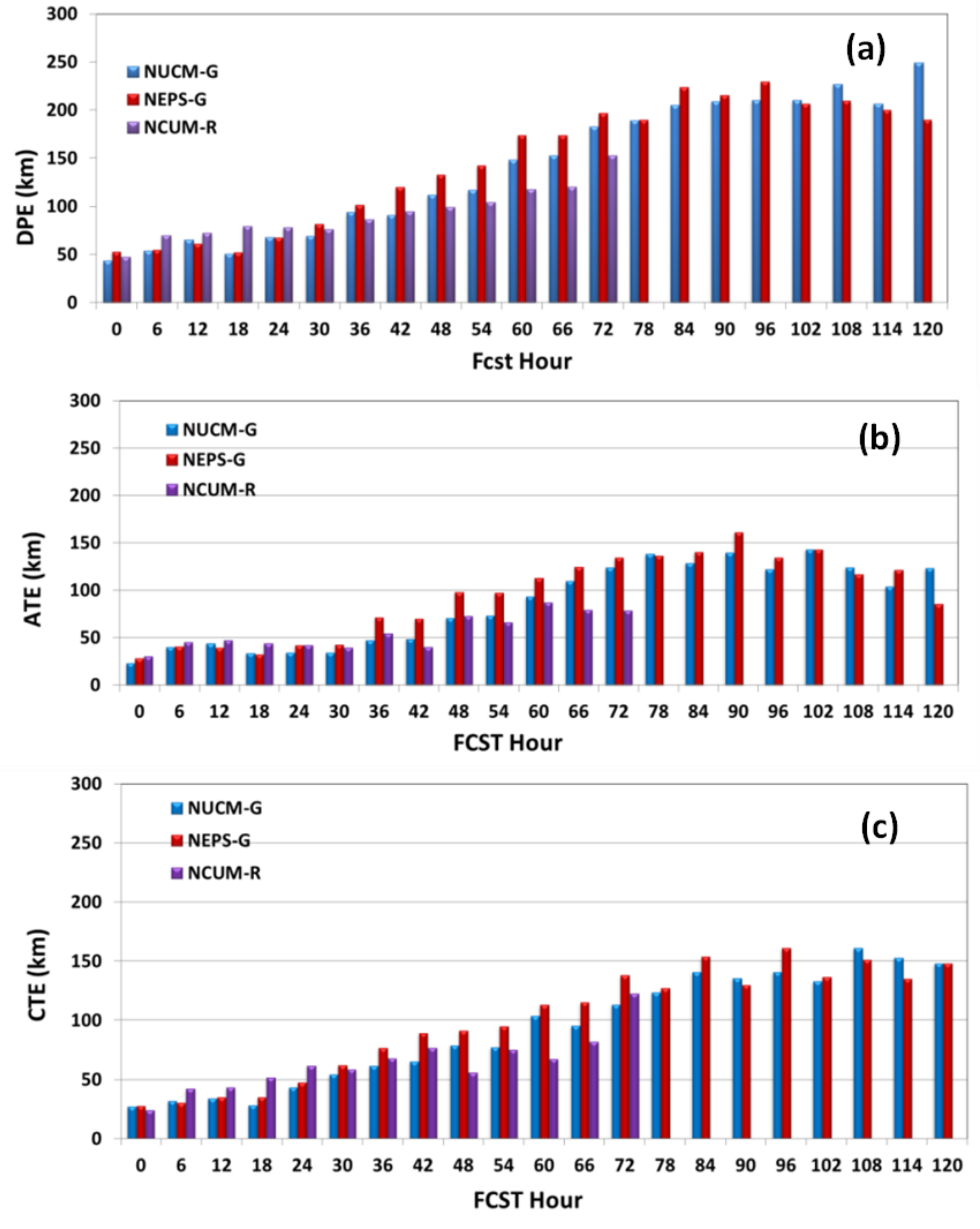

Figure 21: Track forecast errors for cyclone 'Amphan' (13-20 May 2020) (a) Direct position error, (b) along track error and (c) cross track error

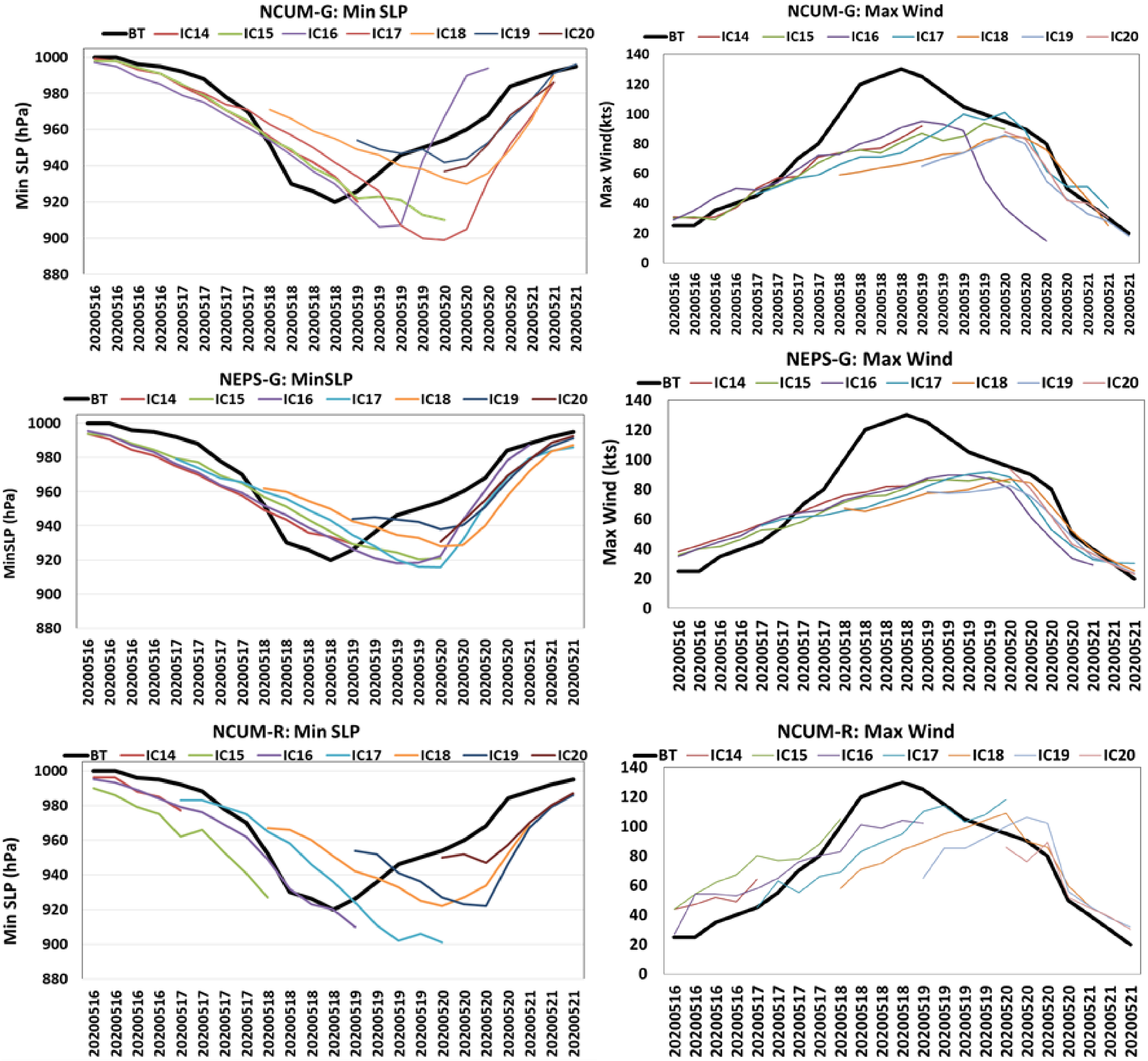

Figure 22: Observed and forecast Minimum SLP (left) and Maximum Wind (right) during 16-21 May 2020

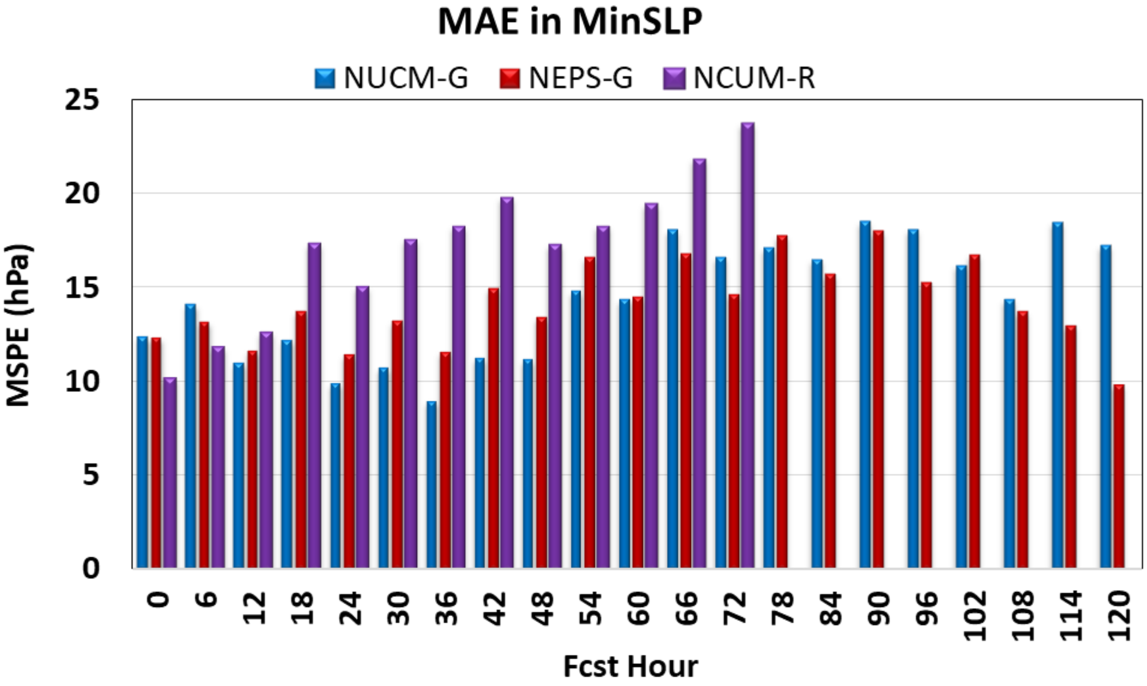

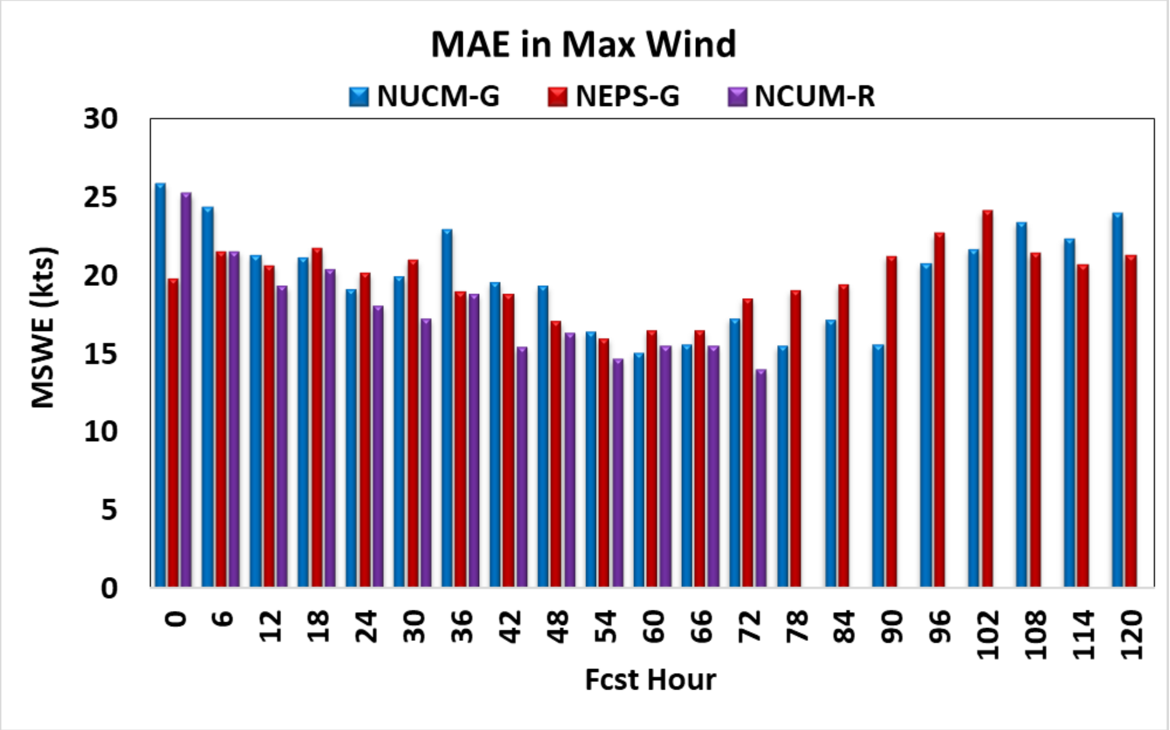

Figure 23: Mean Absolute Error (MEA) in Minimum SLP (top) and Maximum Wind (bottom) at different forecast lead times during 13-20 May 2020

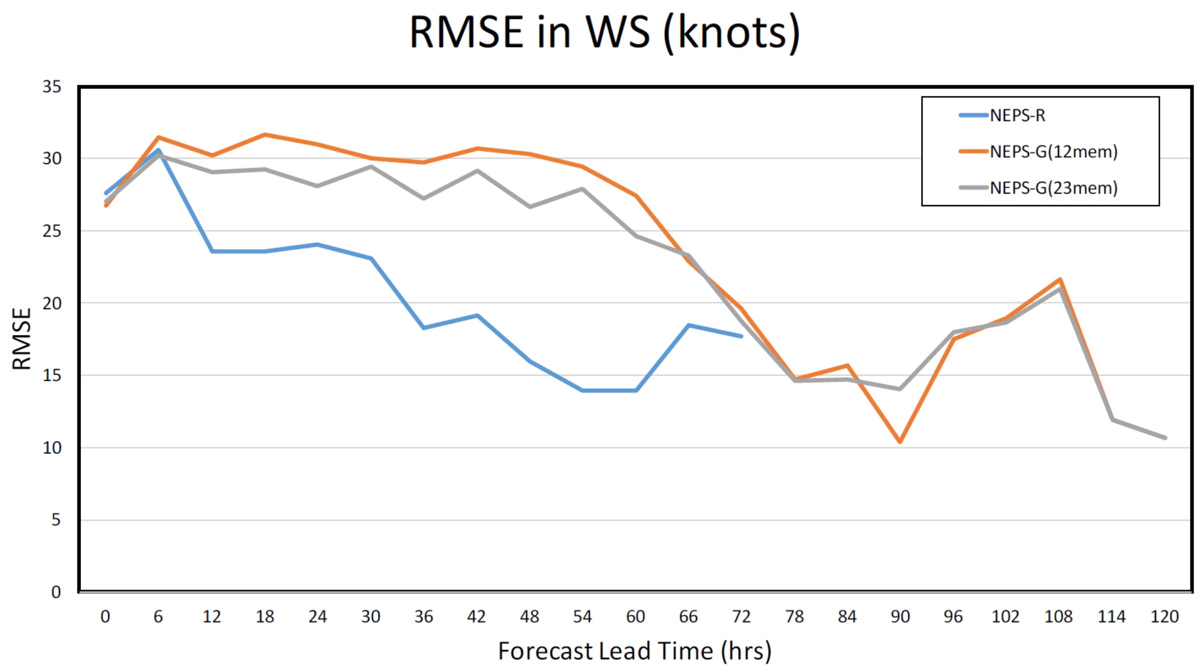

Figure 24: RMSE in forecast Maximum Wind Speed in NEPS-G and NEPS-R at different lead times for cyclone 'Amphan'

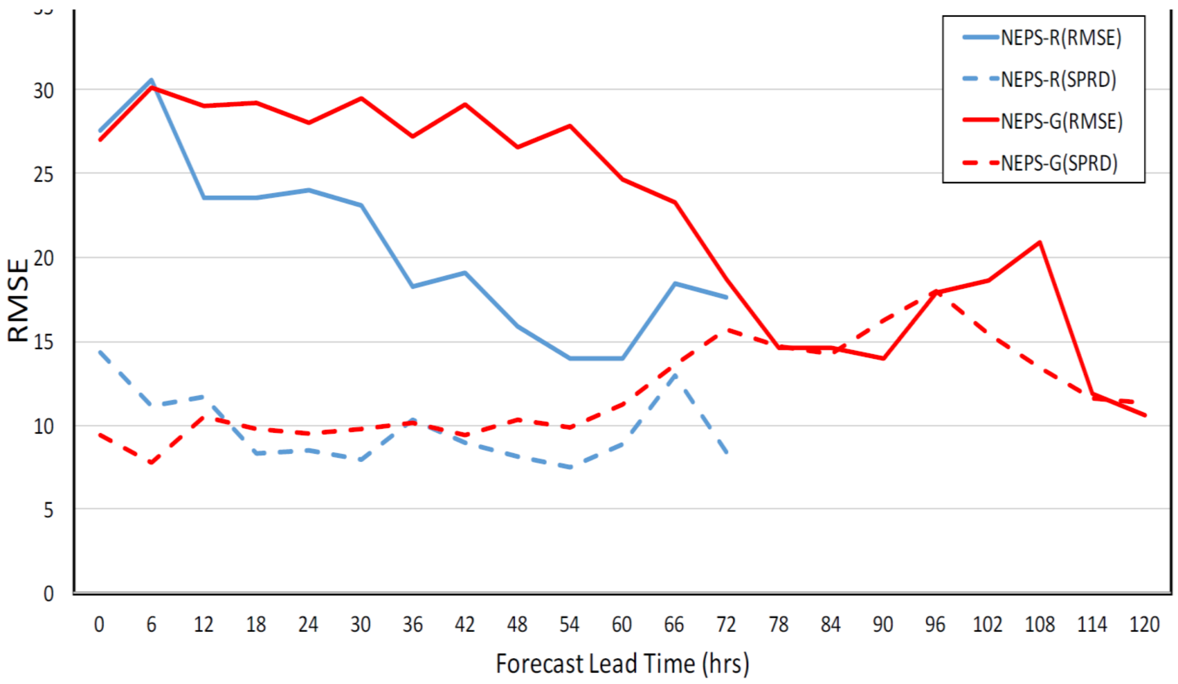

Figure 25: RMSE v/s Spread in forecast Maximum Wind Speed in NEPS-G and NEPS-R at different lead times for cyclone 'Amphan'

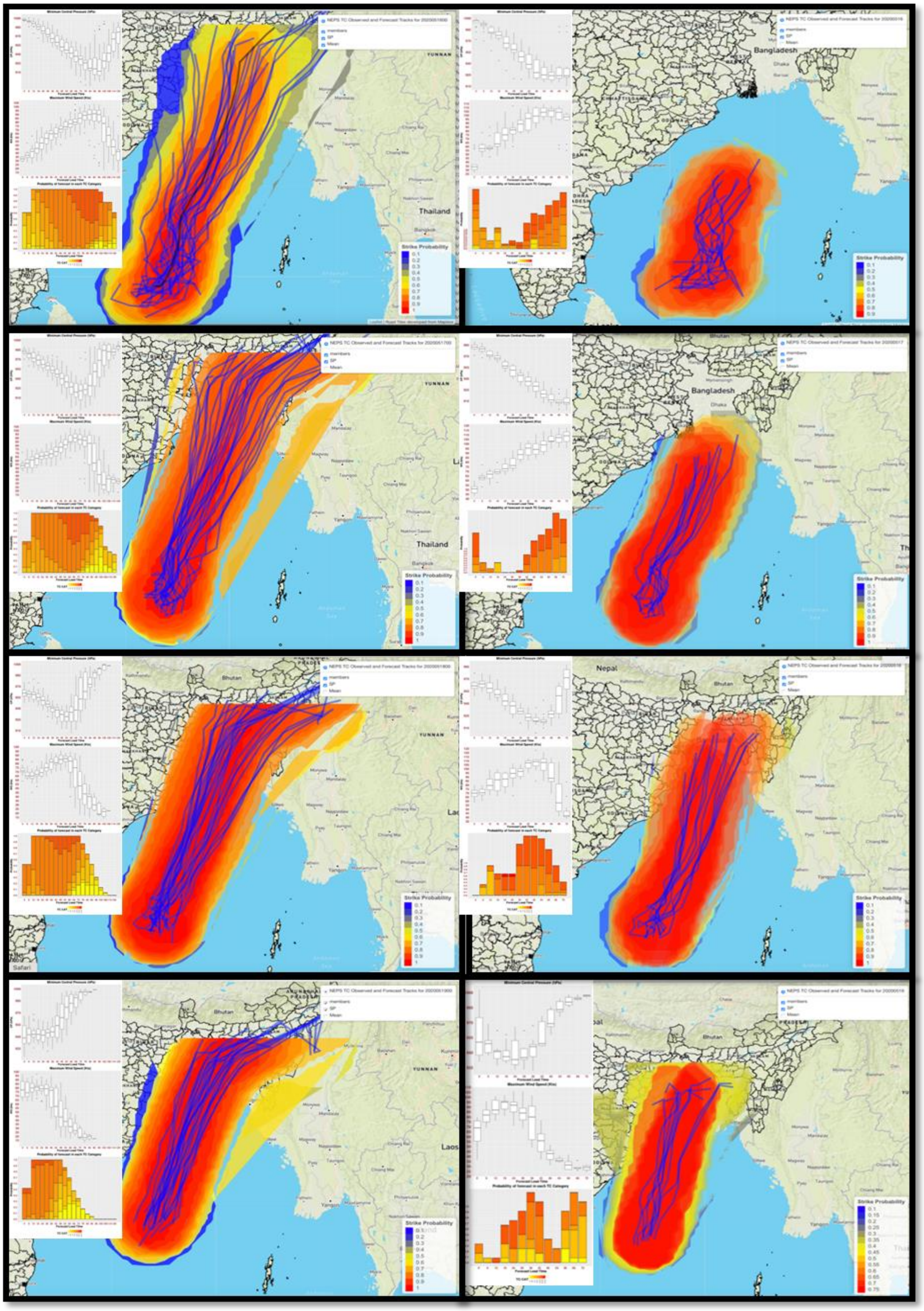

Figure 26: Strike Probability forecasts based on NEPS-G (left) and NEPS-R (right) during 16-19 May 2020

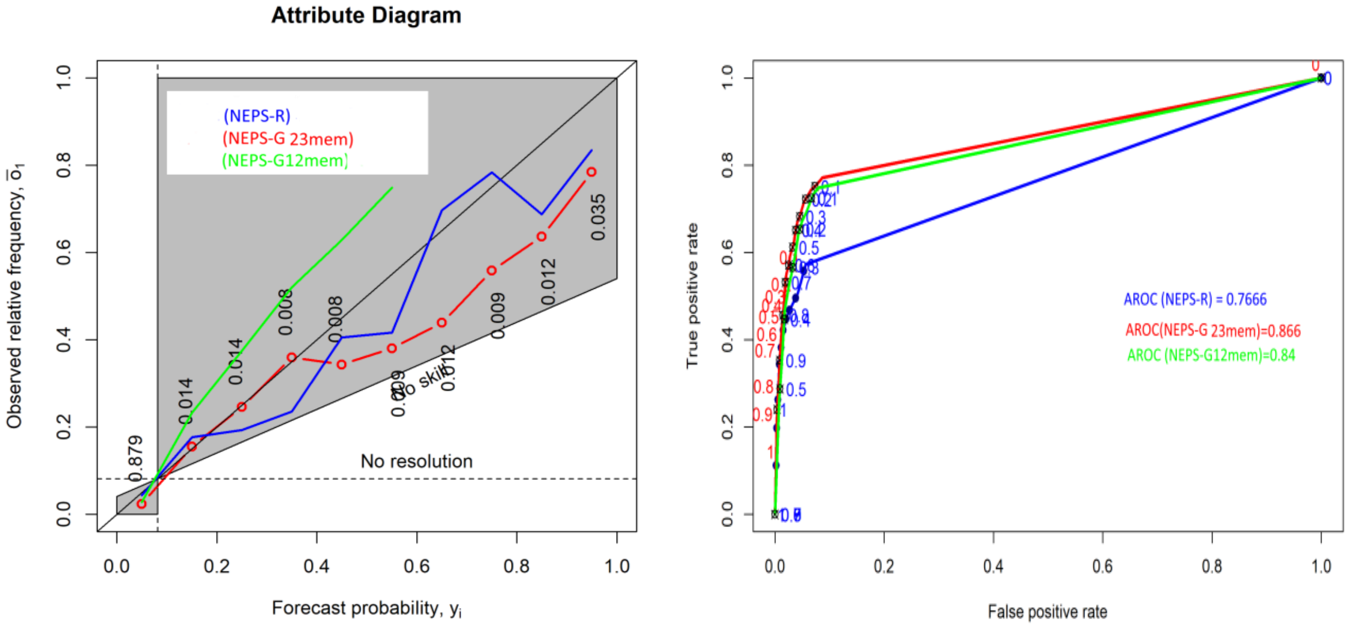

Figure 27: Verification of strike probability using reliability diagram (left) and ROC curve (right) for cyclone 'Amphan' during 16-20 May2020

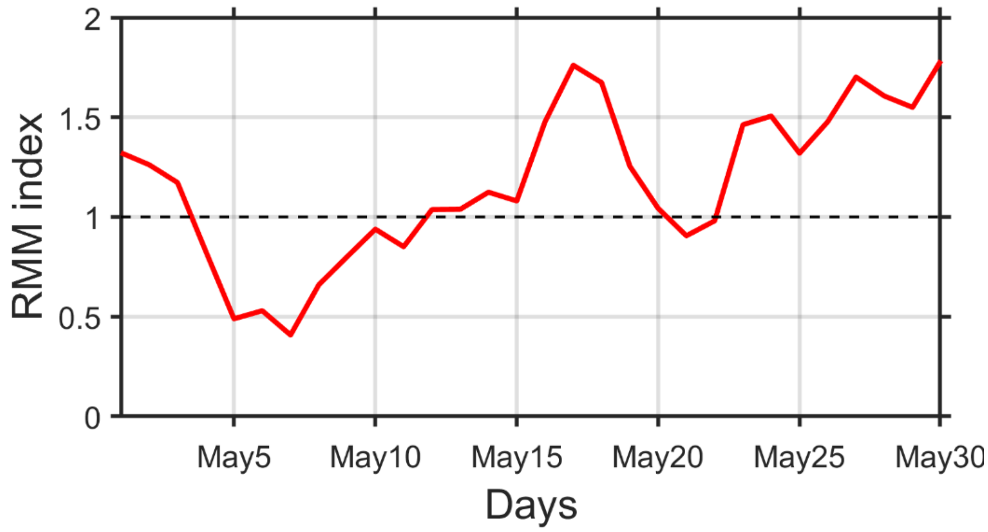

Figure 28 (a): Time series of RMM index during the month of May 2020. The black dashed line indicates the reference RMM amplitude 1. RMM index data is obtained from http://www.bom.gov.au/climate/mjo/

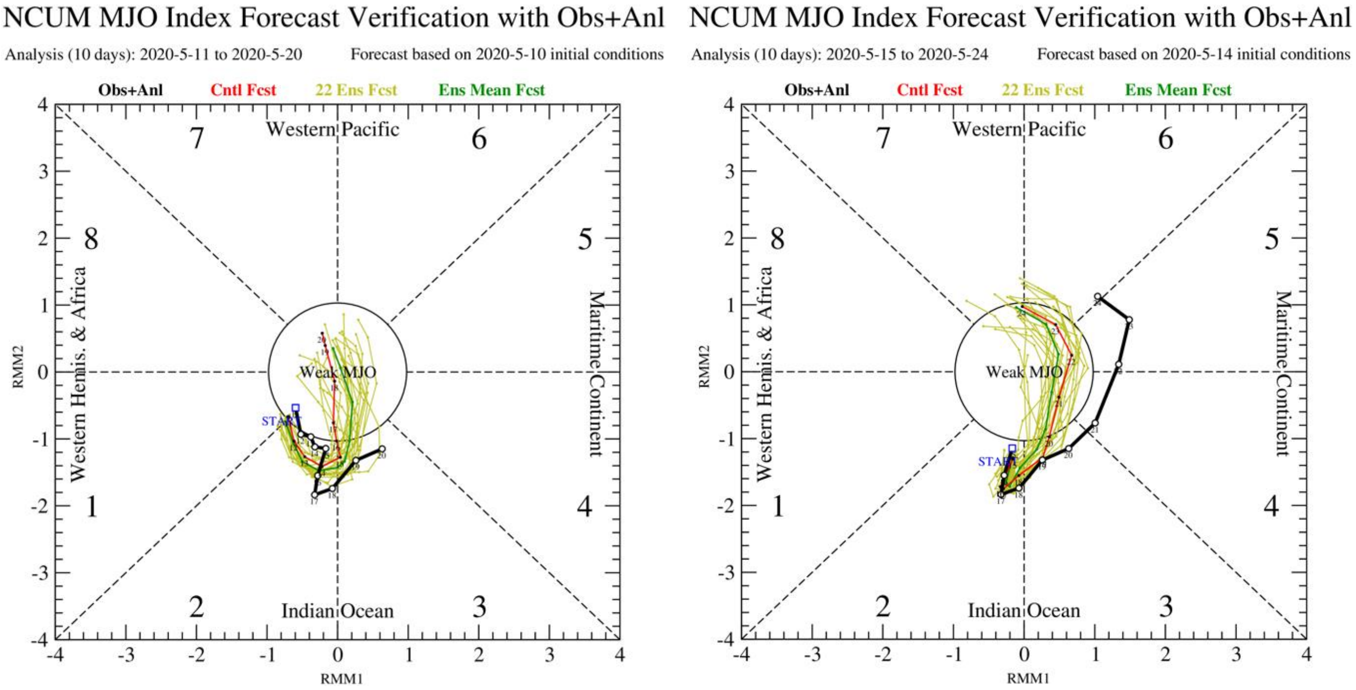

Figure 28 (b) Time series of RMM index during the month of May 2020. The black dashed line indicates the reference RMM amplitude 1 (c) The MJO Index forecast verification during 11-20 May (left) and (c) 15-24 May 2020

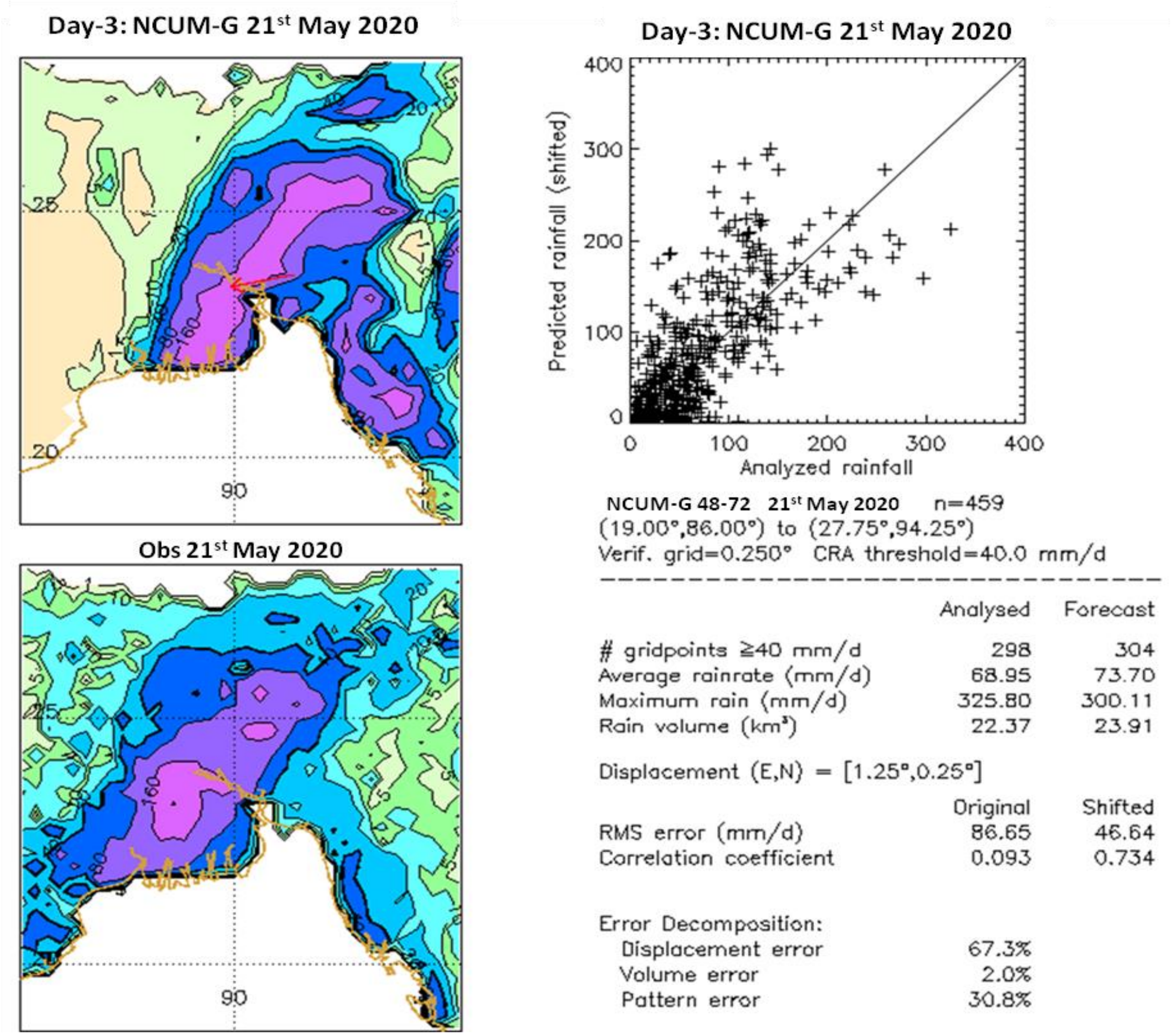

```
NCUM-G 48-72   21st May 2020      n=459
(19.00°,86.00°) to (27.75°,94.25°)
Verif. grid=0.250°  CRA threshold=40.0 mm/d
---------------------------------------------
                                Analysed   Forecast

# gridpoints ≧40 mm/d               298        304
Average rainrate (mm/d)           68.95      73.70
Maximum rain (mm/d)              325.80     300.11
Rain volume (km³)                 22.37      23.91

Displacement (E,N) = [1.25°,0.25°]
                                Original    Shifted
RMS error (mm/d)                  86.65      46.64
Correlation coefficient           0.093      0.734


Error Decomposition:
  Displacement error              67.3%
  Volume error                     2.0%
  Pattern error                   30.8%
```

Figure 29: CRA Verification with 40 mm/day threshold for NCUM-G: Day-3 (upper) and Analysis (lower) rainfall valid on 21th May 2020

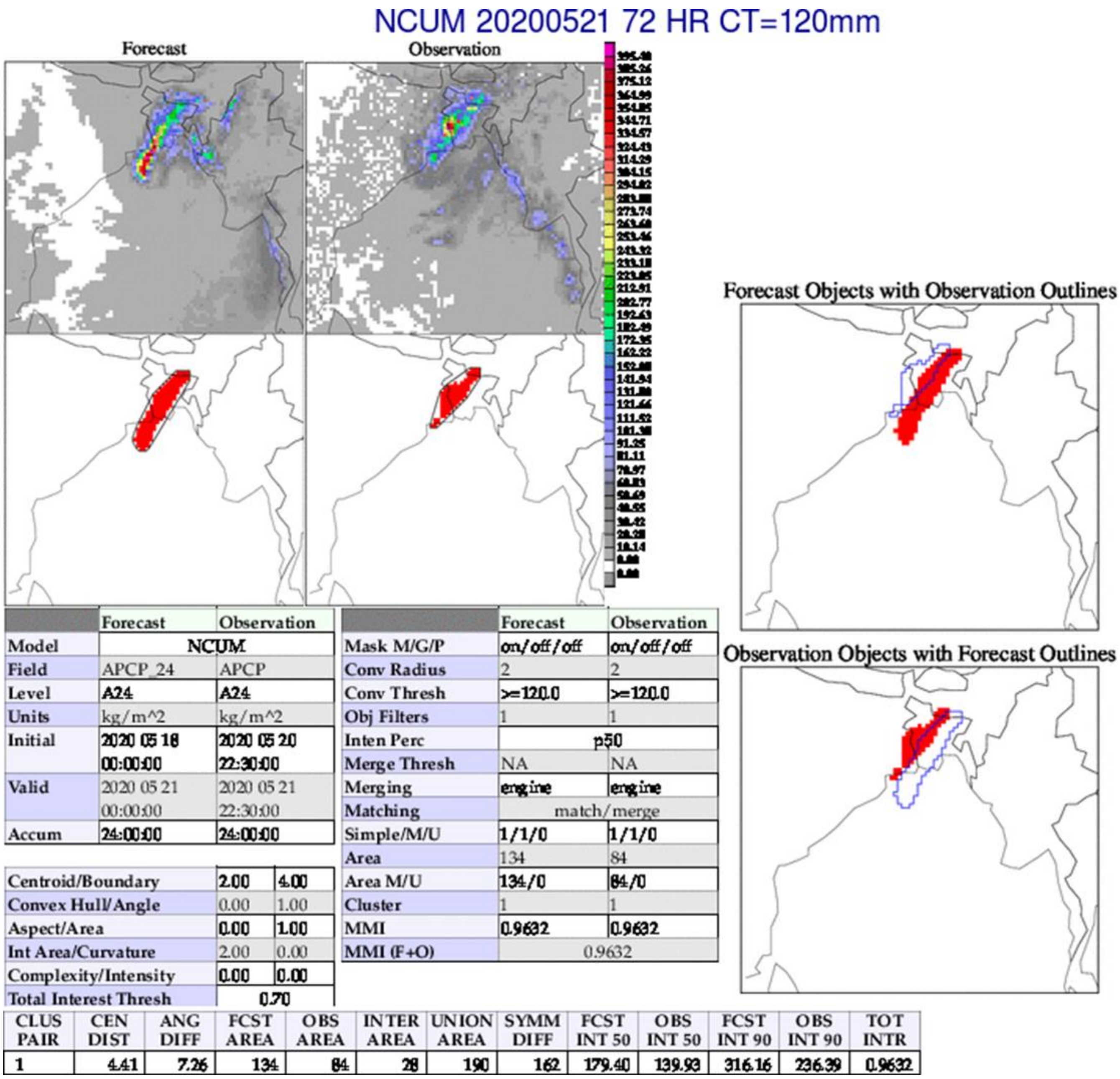

	Forecast	Observation
Model	NCUM	
Field	APCP_24	APCP
Level	A24	A24
Units	kg/m^2	kg/m^2
Initial	2020 05 18 00:00:00	2020 05 20 22:30:00
Valid	2020 05 21 00:00:00	2020 05 21 22:30:00
Accum	24:00:00	24:00:00

Centroid/Boundary	2.00	4.00
Convex Hull/Angle	0.00	1.00
Aspect/Area	0.00	1.00
Int Area/Curvature	2.00	0.00
Complexity/Intensity	0.00	0.00
Total Interest Thresh	0.70	

	Forecast	Observation
Mask M/G/P	on/off/off	on/off/off
Conv Radius	2	2
Conv Thresh	>=120.0	>=120.0
Obj Filters	1	1
Inten Perc	p50	
Merge Thresh	NA	NA
Merging	engine	engine
Matching	match/merge	
Simple/M/U	1/1/0	1/1/0
Area	134	84
Area M/U	134/0	84/0
Cluster	1	1
MMI	0.9632	0.9632
MMI (F+O)	0.9632	

CLUS PAIR	CEN DIST	ANG DIFF	FCST AREA	OBS AREA	INTER AREA	UNION AREA	SYMM DIFF	FCST INT 50	OBS INT 50	FCST INT 90	OBS INT 90	TOT INTR
1	4.41	7.26	134	84	28	190	162	179.40	139.93	316.16	236.39	0.9632

Figure 30: MODE Verification with 120 mm/day threshold for NCUM-G: Day-3 rainfall valid on 21st May 2020

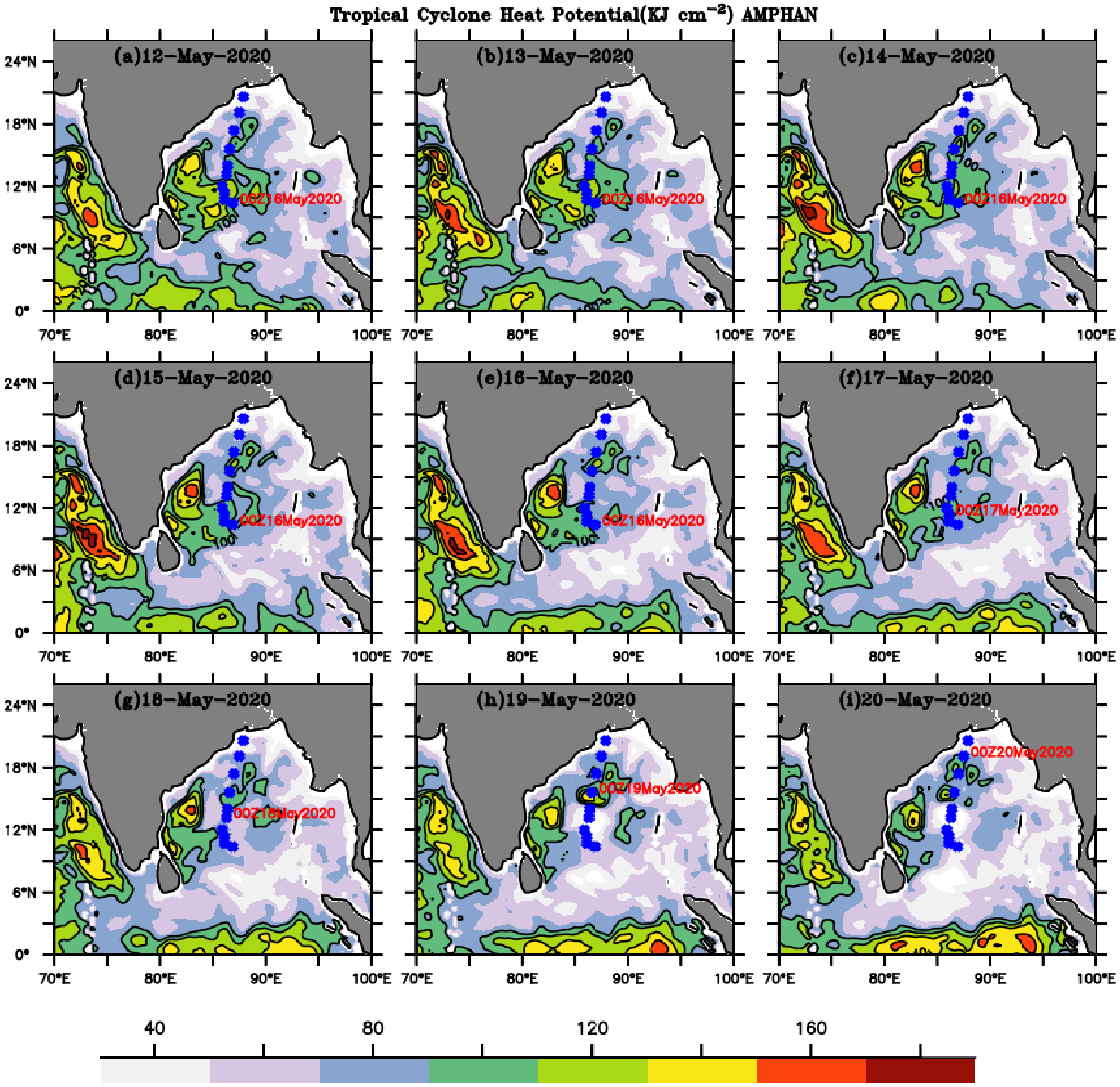

Figure 31: Tropical Cyclone Heat Potential (TCHP; KJcm^{-2}) from the global NEMO ocean analysis during the cyclone Amphan (12-20 May 2020) overlaid the IMD cyclone track